was found to be associated with arterial calcification, especially when patients did not receive sufficient thyroid hormone replacement therapy.[12] However, the mechanism for the calcification in cretins has been to date unclear. A subset of vascular smooth muscle cells, named "calcifying vascular cells," was demonstrated recently to undergo osteogenic and chondrogenic differentiation in culture, indicating that some vascular smooth muscle cells still have the potential for multiple lineages.[13] Because thyroid hormone plays a critical role in bone remodeling,[14] we hypothesized that thyroid hormone is also associated with vascular calcification. To test this hypothesis, we investigated the effect of thyroid hormone on vascular smooth muscle calcification and expression profiles of calcification-associated genes in vitro and in vivo, and identified matrix Gla protein (MGP) gene as a target of thyroid hormone in vascular smooth muscle cells.

Materials and Methods

Cell Culture

α-Actin–positive rat aortic smooth muscle cells (RAOSMCs) were obtained from Cell Applications, Inc. and were cultured on 6-well cell culture plates at 37°C in a humidified atmosphere of 95% air/5% CO_2 in growth medium (GM; Dulbecco's Minimal Essential Medium [DMEM] supplemented with 10% FCS, 100 U/mL penicillin, and 100 μg/mL streptomycin). Cells up to passage 5 were used for the experiments. The culture media were changed every 48 hours. Thyroid hormone–depleted serum was prepared as described previously.[15] To evaluate effects of thyroid hormone on gene expression profiles of the synthetic phenotype of RAOSMCs, the cells at 50% of confluence were cultured in thyroid hormone–depleted medium (TDM; DMEM containing 10% thyroid hormone-depleted serum, 100 U/mL penicillin, and 100 μg/mL streptomycin) for 2 days and stimulated with 3',3,5-triiodo-L-thyronine (T_3) for another 2 days. The contractile form of RAOSMCs was obtained by culturing confluent cells in serum-free differentiation medium (DM; DMEM supplemented with 1× ITS-X (Invitrogen), 5 mmol/L taurine, 100 U/mL penicillin, and 100 μg/mL streptomycin) for 10 days, followed by T_3 treatment for 2 days. The transition of the cell phenotype in DM was confirmed by immunoblotting for nonmuscle myosin heavy chain (SMemb) and smooth muscle myosin heavy chain-2 (SM2). To examine effects of thyroid hormone on calcium accumulation, confluent RAOSMCs were cultured as described previously[16] in TDM with or without 100 ng/mL recombinant human bone morphogenic protein-2 (rBMP2; R & D Systems) in a cell culture dish with or without collagen type IV (Col4) coating (BD Biosciences). Supplementation with β-glycerophosphate, which facilitates smooth muscle cell calcification,[17] was omitted because of a decrease in the signal-to-background ratio. Cells were subsequently stimulated with T_3 for 5 days. The concentrations of free T_3 (fT_3) and free L-thyroxine (T_4) in the serum-containing medium were determined using chemiluminescent enzyme immunoassay at a clinical diagnostic laboratory. The detection limits for fT_3 and fT_4 were 1.1 pmol/L and 1.7 pmol/L, respectively. Human coronary artery smooth muscle cells (HCASMCs; Cell Applications, Inc.) were maintained and transformed into the contractile phenotype before treatment with T_3 by culturing for 7 days in serum-free HCASMC DM (311D-500; Cell Applications, Inc) according to manufacturer instructions.

Animals

Male Sprague-Dawley rats (Japan SLC; Shizuoka, Japan) were maintained on rodent chow (Certified diet MF; Oriental Yeast, Co) and given water ad libitum. For generation of hypothyroid animals, methimazole (MMI; 400 mg/L) was added to the drinking water for 4 weeks. Hyperthyroid rats were generated by daily injection of T_3 (0.2 mg/kg body weight IP) for 10 days. Plasma concentrations of fT_3 and fT_4 were measured, as described above. After the treatment with MMI or T_3, the thoracic aorta was isolated. Animals were 12 weeks old when killed. Aortic smooth muscle tissue for measurements of calcium accumulation and gene expression was cleared of fat, connective tissue, and an endothelium and stored at −80°C until use. For pathological examination, the aortic tissue was fixed in 10% formaldehyde. Transverse aortic sections were taken from the fixed tissue and stained with hematoxylin and eosin. All animals were treated in accordance with laboratory animal care guidelines of National Institute of Health Sciences at Tokyo.

Calcium Accumulation

Calcium content in RAOSMCs and rat aortic smooth muscle tissues were determined as described previously[16] using o-cresolphthalein complexone method. Protein concentration was determined using Bio-Rad protein assay reagent and BSA as a standard.

Real-Time Quantitative RT-PCR

Total RNA was isolated from smooth muscle cells and tissues using Sepasol reagent (Nakalai Tesque) containing 0.1 mg/mL glycogen (Roche Diagnostics) and was treated with DNaseI (Promega) according to the manufacturer protocols. To quantitate specific mRNA levels, the real-time progress of target sequence-specific amplification was monitored during RT-PCR using TaqMan chemistry and PRISM7000 Sequence Detection System (Applied Biosystems). An 18S ribosomal RNA was used as an internal control for each RNA level. Sequences of the primers and the TaqMan probes are listed in supplemental Table I (available online at http://circres.ahajournals.org).

Western Blot Analysis

RAOSMCs and aortic smooth muscle tissues were homogenized in lysis buffer as described previously.[18] After measuring protein concentrations, proteins were separated by SDS-PAGE and blotted onto polyvinylidene fluoride membranes, which were incubated with anti-SMemb or anti-SM2 monoclonal antibodies (Yamasa) or an anti-MGP polyclonal antibody (TransGenic) for 1 hour at room temperature. Subsequently, membranes were incubated with the secondary antibody conjugated with horseradish peroxidase for 1 hour. Signals were visualized and quantified using ECL Plus system (Amersham Biosciences) and LAS-3000 Imaging System (FUJIFILM), respectively.

Promoter Activity Assay

Fragments between −1752 and −1 of 5' flanking sequence of the MGP gene exon 1 and between −1895 and −1 of 5' flanking sequence of the stanniocalcin-1 (STC1) gene exon 1 were amplified using rat tail genomic DNA as a template. The primers for PCR amplifications were designed as based on the nucleotide sequences (MGP forward: CAAGGGTACCGGTTTGAGAGACCACGAGAC; MGP reverse: CTTGAAGCTTCCTGTGAGTCTGCCTCTGTG; STC1 forward: CAAGCTCGAGCCCCTGATATTTCAGCATGG; STC1 reverse: CTTGAAGCTTAGGTGAGGATTTGAGGAGG). The amplicons were subcloned into the firefly luciferase expression vector pGL3-Basic (Promega). RAOSMCs in the contractile state, grown on a 24-well plate, were transiently cotransfected with 225 ng/well of each promoter luciferase plasmid and 75 ng/well of phRL-TK control plasmid (Promega) using FuGene6 (Roche). Three hours after transfection, cells were incubated with or without T_3. The luciferase activity was defined as a ratio of the firefly luciferase signal to the renilla luciferase signal, which was measured with Dual-Luciferase Reagent (Promega). The transfection efficiency of the plasmids was estimated to be 1% to 10% of the total RAOSMCs, as assessed by transfection experiments with an enhanced green fluorescent protein expression vector pEGFP-N1 (BD Biosciences Clontech; data not shown).

RNA Interference Against TRα

RAOSMCs in the synthetic form were transiently transfected with StealthRNAi (Invitrogen) specific for TRα gene (sense: CCAGAAGAACCUCCAUCCCACCUAU; antisense: AUAGGUGGGAUG-

Free Thyroid Hormone Concentrations in Rat Plasma and Serum-Containing Cell Culture Medium

Plasma/Medium	fT_3 (pmol/L)	fT_4 (pmol/L)	Calculated Range of Thyroid Hormone Activity (pmol fT_3/L)
Plasma from a euthyroid rat	4.2±0.6	27±2	6.9–31
Plasma from a hypothyroid rat (MMI treatment for 1 month)	<1.1	<1.8	<1.3–2.9
GM (DMEM, 10% FCS, P/S)	3.7±0.2	15±0.0	5.2–19
TDM (DMEM, 10% thyroid hormone–depleted FCS, P/S)	<1.1	2.7±0.2	<1.4–3.8
TDM (DMEM, 10% thyroid hormone–depleted FCS, P/S) + 1 nmol/L T_3	15±1*	3.4±0.1*	15–18

The range of thyroid hormone activity was calculated assuming that X% (X=0–100) of T_4 is processed to T_3 at the site of action in vivo and that the affinity of T_4 for TRs is one tenth that of T_3.

P/S indicates penicillin and streptomycin.

Values are means±SD; *P<0.05 vs TDM without T_3 supplementation (Student t test).

GAGGUUCUUCUGG) or StealthRNAi negative control medium GC (Invitrogen) using Lipofectamine 2000 (Invitrogen), according to manufacturer instructions and incubated in TDM for 2 days. Cells were then treated with or without T_3 (15 pmol/L fT_3) for another 2 days. Total RNA was isolated from cells before and after T_3 treatment for mRNA determinations.

Statistics

Data were expressed as means±SEM unless otherwise indicated. Data were analyzed for statistical significance by Student t test or ANOVA with Student-Newman-Keuls test as a post hoc test. Significance was imparted at the P<0.05 level.

Results

Free Thyroid Hormone Concentrations

As shown in the Table, plasma concentrations of fT_3 and fT_4 in euthyroid rats were 4.2±0.6 pmol/L and 27±2 pmol/L (mean±SD), respectively. The MMI treatment decreased fT_3 and fT_4 to <1.1 pmol/L and to <1.8 pmol/L, respectively, indicating that the animals were hypothyroid. The fT_3 and fT_4 levels in GM containing 10% FCS were 3.7±0.2 pmol/L and 15±0.0 pmol/L (mean±SD), respectively, and happened to be similar to those in plasma from euthyroid rats. The free concentrations of thyroid hormones in TDM (<1.1 pmol/L fT_3; 2.7 pmol/L fT_4) were low enough to keep TRs inactivated because the K_d values of T_3 for TRs are known to be ≈10 to 100 pmol/L[19] and because T_4 has ≈10-fold lower affinity for TRs than that of T_3. In vascular smooth muscle cells, T_4 is known to be converted to T_3 by type II iodothyronine deiodinase,[10] although the conversion rate in vivo is not clear. Assuming that X% (X=0 to 100) of T_4 is processed to T_3 at the site of action in vivo and that the affinity of T_4 for TRs is one tenth of that of T_3, the total activity of thyroid hormones in euthyroid rat plasma should be equivalent to that of 6.9 to 31 pmol/L [4.2+27×X/100+27×(1−X/100)/10] of fT_3 alone. The supplementation of T_3 to TDM at 1 nmol/L of total concentration resulted in an increase in fT_3 to 15±1 pmol/L (mean±SD), with a slight increase in fT_4, therefore, it was regarded within a euthyroid range.

T_3-Induced Gene Expression and Calcification in Cultured RAOSMCs

Vascular smooth muscle cells show a high degree of plasticity and are able to interchange between a differentiated, contractile phenotype and a proliferating, synthetic phenotype. Therefore, we first examined the effects of T_3 on expression profiles of calcification-associated genes in both phenotypes. RAOSMCs in GM predominantly expressed a marker of synthetic phenotype: SMemb. The replacement of the medium with DM reduced the protein level of SMemb to 28% and increased SM2 expression by 11.6-fold (online Figure I), indicating the transition of the phenotype. In the synthetic phenotype, T_3 (1 nmol/L total T_3=15 pmol/L fT_3) led to upregulation of mRNAs for MGP and STC1×3.3-fold and 1.3-fold, respectively (Figure 1A), whereas osteopontin

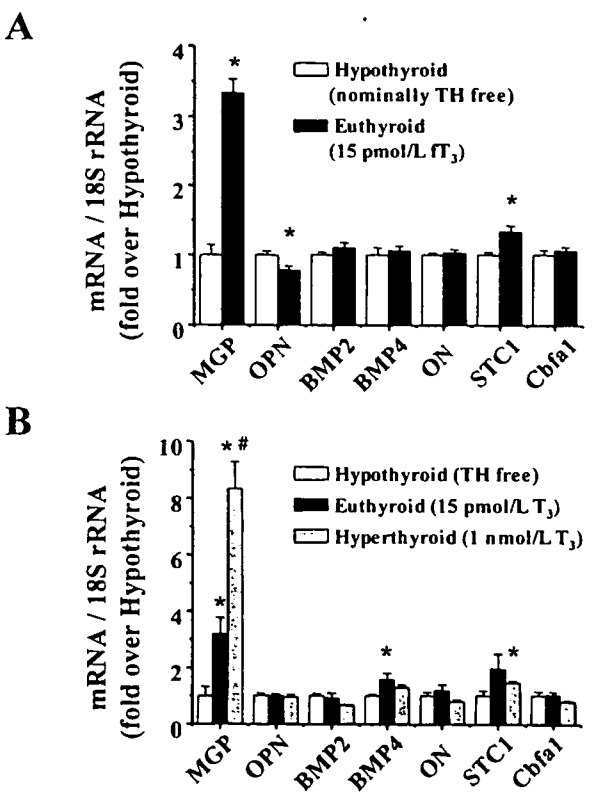

Figure 1. T_3 regulated expression of calcification-associated genes in cultured RAOSMCs in synthetic and contractile forms. A, Effect of T_3 on mRNA expression of calcification-associated genes in the synthetic form of RAOSMCs cultured in TDM. Cells were treated with 15 pmol/L fT_3 for 2 days. B, Effect of T_3 on mRNA expression of calcification-associated genes in the contractile form of RAOSMCs cultured in the DM. Cells were treated with 15 pmol/L or 1 nmol/L T_3 for 2 days. Values are expressed as means±SEM (n=4) TH indicates thyroid hormone. *P<0.05 vs hypothyroid; #P<0.05 vs euthyroid.

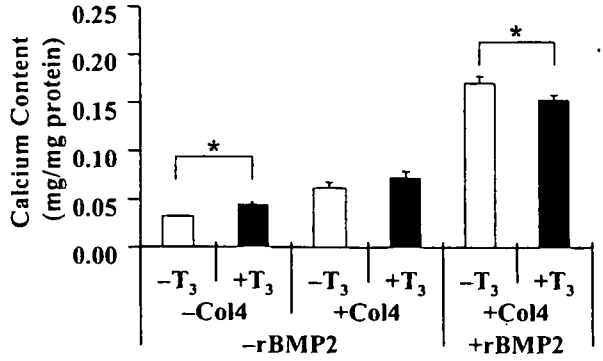

Figure 2. Effects of T_3 on calcium accumulation in cultured RAOSMCs. The confluent cells cultured in TDM were stimulated by 15 pmol/L fT_3. In the absence of rBMP2, T_3 significantly increased calcium content in RAOSMCs cultured in noncoated vessels. Supplementation with rBMP2 increased the basal calcium content in RAOSMCs in Col4-coated vessels and reversed the effect of T_3 on the calcification. Values are expressed as means±SEM (n=6 to 8); *$P<0.05$.

(OPN) was downregulated by 21%. The mRNA levels of BMP2, bone morphogenic protein-4 (BMP4), osteonectin (ON), and core binding factor α1 (Cbfa1; also known as Runx2 or Osf2) were not significantly altered by the T_3 treatment. Specific signals for osteocalcin and bone sialoprotein mRNA were not detected by several independent primer sets in all experiments of the present study, presumably because of their low abundance in vascular smooth muscle cells. In the contractile phenotype in DM, T_3 (15 pmol/L) induced upregulation of MGP and BMP4×3.2-fold and 1.6-fold, respectively (Figure 1B). A higher concentration of T_3 (1 nmol/L) resulted in a further increase in the MGP mRNA level and a significant upregulation of STC1 mRNA, indicating the dose dependency of the effects. Messenger RNA levels of OPN, BMP2, ON, STC1, and Cbfa1 in the contractile phenotype were not significantly altered by the T_3 treatment. Among the calcification-associated genes, MGP and STC1 genes were commonly upregulated by T_3 in both phenotypes, suggesting that these two genes were relatively essential in RAOSMCs as targets of thyroid hormone.

Because the effect of MGP on calcification and osteogenic differentiation of vascular smooth muscle cells depends on availability of BMP2 and Col4,[20,21] cell calcification was determined in the absence or presence of these factors. In the absence of rBMP2 and Col4 coating, treatment with T_3 (1 nmol/L total T_3=15 pmol/L fT_3) for 5 days resulted in an increase in calcium content by 39% in RAOSMCs (Figure 2). The same treatment tended to have the similar effect on cells in a Col4-coated vessel in the absence of rBMP2. In contrast, T_3 led to a significant decrease in cellular calcium by 10% in the presence of rBMP2 and Col4-coating.

Transcriptional Regulation of MGP and STC1 Genes by T_3

To test a hypothesis that the promoters of MGP and STC1 genes were under regulation of thyroid hormone, RAOSMCs were transiently transfected with luciferase reporters under control of the MGP and STC1 promoters. The 5′ flanking sequences of MGP and STC1 genes have been submitted to

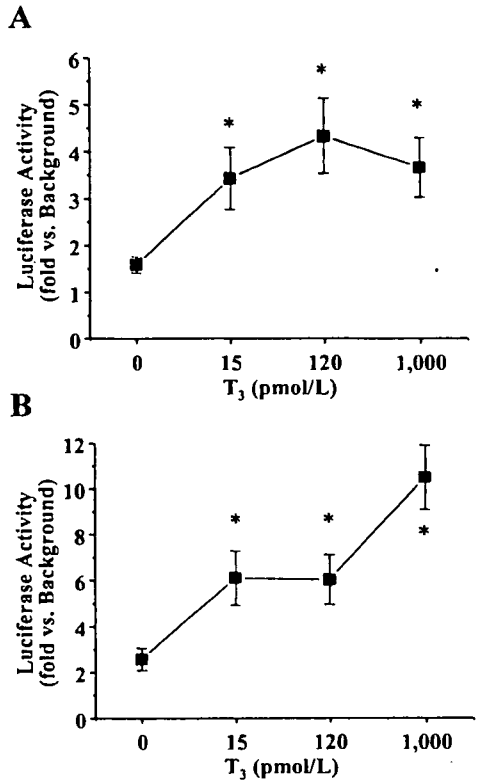

Figure 3. T_3 activated luciferase reporter genes driven by rat MGP (A) and STC1 (B) promoters in the contractile form of RAOSMCs. Cells were transiently cotransfected with a reporter plasmid containing a promoter region of rat MGP or STC1 gene and an internal control plasmid (phRL-tk) and were treated with T_3 for 2 days. The cell extracts were assayed for luciferase activity. Values are normalized to the background (luciferase activity of the cells transfected with promoterless pGL3-Basic vector and phRL-tk) and expressed as means±SEM (n=6); *$P<0.05$ vs control.

NCBI (accession numbers AY750958 and AY750959, respectively). Transcription Element Search System (TESS)[22] revealed that consensus sequences of the thyroid hormone response element were located in 585 to 600 (*TGTACCCCAATGAACC*) and 1009 to 1024 (*TGGAGACAGGAGGACA*) bases upstream of the putative transcription initiation sites of MGP and STC1 genes, respectively. Treatments of the cells with T_3 (15 pmol/L to 1 nmol/L) for 48 hours resulted in significant increases in transcriptional activity compared with vehicle treatment (Figure 3).

Regulation of MGP and STC1 Expression via TRs

Arterial smooth muscle cells express TRα1 and TRα2 nuclear receptor isoforms strongly and TRβ1 and TRβ2 relatively weakly.[10] To evaluate the involvement of TRs in the T_3-induced upregulation of MGP and STC1 mRNAs, RNA interference (RNAi) was performed using StealthRNAi specific for the TRα gene encoding TRα1 and TRα2. The RNAi in RAOSMCs for 2 days significantly attenuated mRNA expression of TRα1 and TRα2 by 66% and 57%, respectively, compared with the controls (Figure 4). The RNAi was also associated with upregulation of MGP mRNA by 32%

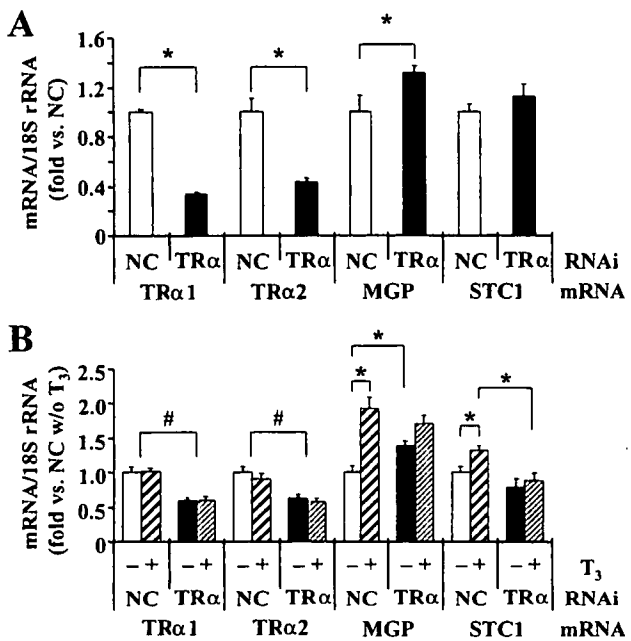

Figure 4. The RNAi against TRα gene in RAOSMCs (synthetic form). A, RNAi against TRα gene for 2 days led to significant decreases in expression of TRα1 and TRα2 to the same extent and a slight increase in the MGP expression. B, The expression of TRα1 and TRα2 remained reduced after the following incubation for 2 more days and was not altered by T_3 (15 pmol/L fT_3). The RNAi was associated with loss of responsiveness of MGP and STC1 mRNA to T_3. Values are expressed as means±SEM (n=4 to 6 [A] and 8 [B]). NC indicates negative control. *$P<0.05$ (Student t test [A] or Student-Newman-Keuls test [B]); #$P<0.05$ association with RNAi (two-way ANOVA).

compared with the controls, suggesting that unliganded TRα1 or TRα2, which has no affinity for thyroid hormones, had an inhibitory effect on the expression of MGP. The mRNA level of STC1 was not altered by the RNAi. Incubation with 15 pmol/L fT_3 for the following 2 days facilitated the expression of MGP and STC1 in the control group, whereas no significant effect of T_3 on MGP and STC1 gene expression was detected in the RNAi group. T_3 had no effect on the expression of the TRα isoforms.

Calcium Accumulation in Hypothyroid Rat Aorta

As examined by hematoxylin-eosin staining, the cross-sections of aorta from rats treated with MMI for 4 weeks did not show obvious calcified foci (Figure 5A). However, *o*-cresolphthalein complexone experiments indicated that the 4-week treatment with MMI significantly increased the calcium content in the rat aortic smooth muscle tissues by 33% compared with that of euthyroid animals (Figure 5B). Quantitative RT-PCRs revealed that mRNA levels of MGP, BMP4, ON, and Cbfa1 were downregulated by 68%, 87%, 69%, and 72%, respectively, by the MMI treatment. OPN, BMP2, and STC1 mRNA levels were not significantly altered (Figure 5C). MMI also attenuated protein expression of MGP by 54% (Figure 5D). Calcified foci were not observed even in aortic cross-sections from rats treated with MMI for 12 weeks (online Figure II), suggesting that the calcification was not progressive.

Calcium Content in Hyperthyroid Rat Aorta

Hyperthyroidism elicits pronounced vascular relaxation.[9] However, the effect of hyperthyroidism on vascular calcification has been unclear. Therefore, it is of interest to compare effects of hyperthyroidism on the expression profiles of calcification-associated genes with those of hypothyroidism. In contrast to the aortic smooth muscle from hypothyroid rats, daily injections of T_3 for 10 days led to a decrease in the calcium content in the rat aortic smooth muscle tissues by 11% compared with that of euthyroid animals (Figure 6A). Quantitative RT-PCRs showed that mRNA levels of MGP, OPN, and BMP2 were upregulated by 4.5-fold, 4.9-fold, and 3.4-fold, respectively, by the T_3 treatment, whereas hyperthyroidism resulted in a significant decrease in the level of STC1 mRNA (Figure 6B).

Upregulation of MGP mRNA in Cultured HCASMCs

To demonstrate that thyroid hormone regulates MGP gene expression in vascular smooth muscle cells of a different species, we determined MGP mRNA levels in HCASMCs in the presence and absence of T_3. Treatment with a physiological concentration (15 pmol/L) of T_3 for 2 days led to a significant increase in MGP mRNA by 40% (1.0±0.07 [hypothyroid 0 pmol/L T_3] versus 1.40±0.13 [euthyroid 15 pmol/L T_3] in an arbitrary unit; n=12).

Discussion

In the present study, thyroid hormone led to an upregulation of MGP in arterial smooth muscle cells in vitro regardless of culture condition, phenotype, and animal species of the cells. The transcriptional activity of the MGP gene was increased by T_3, and reduction of TRα gene expression led to a loss of responsiveness of the MGP gene to T_3, suggesting that the effect of T_3 is based on a genomic action via TRα1. Furthermore, in vivo hormone levels were positively and negatively associated with the expression of MGP and calcification in vascular smooth muscle, respectively. Because aortic smooth muscle from hypothyroid rats showed no obvious neointimal formation, the vascular calcification under the hypothyroidism is likely to be similar to that of media sclerosis. In aortic smooth muscle from hypothyroid rats, expression levels of calcification activators BMP4, ON, and Cbfa1 were decreased, whereas hyperthyroidism upregulated another calcification activator BMP2. However, calcium content in aortic smooth muscle was increased in hypothyroidism, and the opposite was observed in hyperthyroidism, suggesting that the expression or function of calcification inhibitors, such as MGP and OPN, are more dominant for the phenotypic outcome in vivo, compared with those of the calcification activators.

MGP is a mineral-binding extracellular matrix protein synthesized by vascular smooth muscle cells and chondrocytes. Luo et al have shown that ablation of MGP gene in mice causes extensive and lethal calcification and cartilaginous metaplasia of the media of all elastic arteries, indicating that MGP has an inhibitory effect on media calcification in vivo.[23] In contrast, in the same study, morphological analysis showed that heterozygous MGP knockout mice, which had a

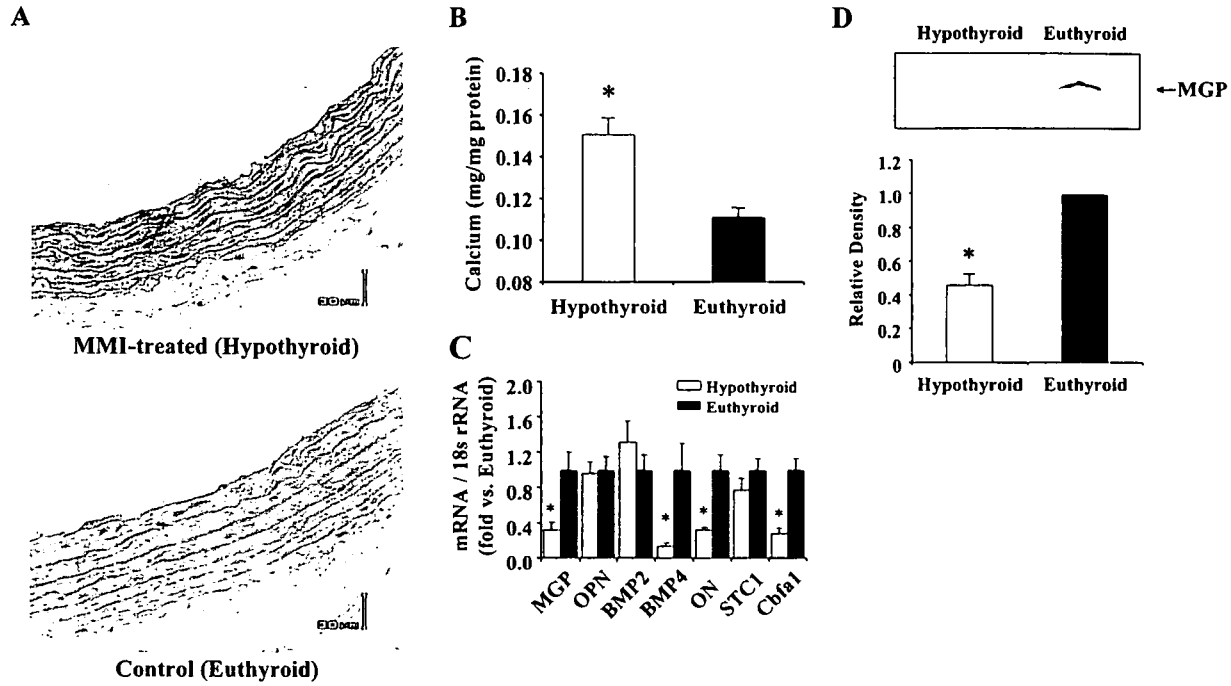

Figure 5. Hypothyroidism led to calcium accumulation in aortic smooth muscle and an altered expression profile of calcification-associated genes. Hypothyroidism was achieved by treatment of the animals with MMI (400 mg/L drinking water) for 4 weeks. A, Hematoxylin-eosin staining of cross-sections of aortae from euthyroid and hypothyroid rats. No obvious calcified foci were observed in either section. Bar=30 μm. B, Effect of the hypothyroidism on calcium deposition in rat aortic smooth muscle. C, Effect of hypothyroidism on mRNA expression of calcification-associated genes in rat aortic smooth muscle. D, Effect of hypothyroidism on MGP protein expression in rat aortic smooth muscle. Values are expressed as means±SEM (n=7 to 8); *$P<0.05$ vs euthyroid.

similar decrease in an arterial MGP level to that by the MMI treatment in the present study, had no obvious calcified foci in arterial smooth muscle. However, this does not necessarily imply that the heterozygous ablation of MGP gene does not affect calcium content in arteries because biochemical quantification for tissue calcium has not been performed. Thus, it is still possible that there is a dose-response relationship between MGP and media calcification, and that an ≈50% reduction of MGP results in some increase in calcium content, although it may not be morphologically evident.

The extracellular environment around smooth muscle cells is known to determine a functional role of MGP. Namely, calcification of vascular smooth muscle cells in the presence of a relatively high concentration of BMP2 was inhibited by MGP, whereas calcification of vascular smooth muscle cells under a low concentration of BMP2 was stimulated by MGP.[20] Moreover, extracellular matrix proteins, especially Col4, have significant influence on MGP function and vascular calcification.[21] In fact, the effect of T_3 on calcification of RAOSMCs was determined by these environmental factors. Therefore, these results suggest that T_3 regulates smooth muscle cell calcification, at least partly, by promoting MGP expression, although not only vascular cells but also migratory adventitial pericytic myofibroblasts and circulating skeletal progenitors may have some additional contributions to vascular calcification in vivo.[24]

STC1 is a mammalian homolog of stanniocalcin, the fish calcium/phosphate- regulating polypeptide that inhibits calcium flux into cells and stimulates phosphate reabsorption. In the present study, gene transcription of STC1 appeared to be regulated by T_3 via TRα in a dose-dependent manner. However, the highest mRNA expression of STC1 tended to be achieved at a euthyroid status in vitro and in vivo, and hyperthyroidism significantly attenuated the STC1 mRNA expression in vivo. Recently, STC1 was shown to accelerate osteoblast development in an autocrine/paracrine manner in cultured fetal rat calvaria cells.[25] Therefore, the downregulation of STC1 may also contribute to the low calcium content in aortic smooth muscle of hyperthyroid rats, although the mechanism that offsets the increase in the STC1 gene transcription remains to be elucidated.

OPN is known to inhibit or promote vascular smooth muscle calcification in vivo in a phosphorylation-dependent manner.[26] Therefore, the changes in its expression in the synthetic form of RAOSMCs and in smooth muscle tissue of hyperthyroid rats may be also associated with the effect of thyroid hormone on calcium accumulation. However, as shown in the in vitro and MMI experiments, a physiological concentration of thyroid hormone is unlikely to target OPN gene directly, at least in the contractile form of aortic smooth muscle cells.

BMP2 was upregulated by hyperthyroidism in vivo, whereas BMP4 was downregulated by MMI-induced hypothyroidism. BMP2 is know to antagonize the effect of MGP,[20] and BMP4 has been suggested to play a significant role as a cytokine, a growth factor or a media-calcification promoter in vascular lesions of calciphylaxis.[27] The mRNA levels of ON and Cbfa1 were also decreased in hypothyroid rat aortic smooth muscle. With the exception of BMP4, these changes in vivo did not follow on from the in vitro experiments,

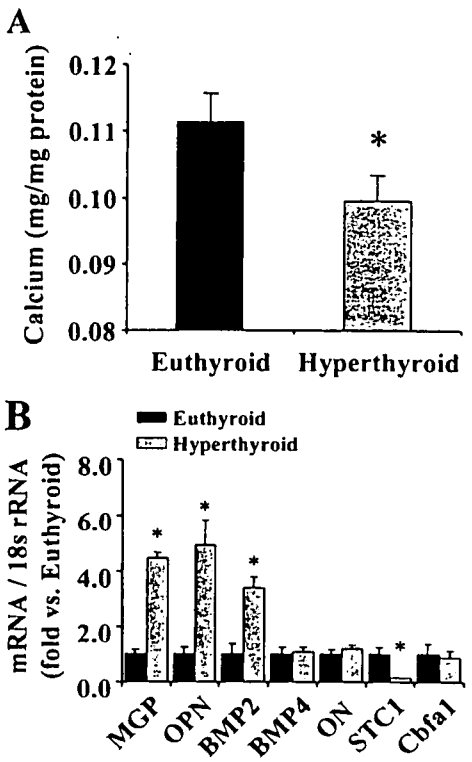

Figure 6. Hyperthyroidism decreased tissue calcium content in aortic smooth muscle and altered the expression profile of calcification-associated genes. Hyperthyroidism was achieved by daily injection of T_3 (0.2 mg/kg body weight IP) for 10 days. A, Effect of the hyperthyroidism on calcium deposition in rat aortic smooth muscle. C, Effect of hyperthyroidism on mRNA expression of calcification-associated genes in rat aortic smooth muscle. Values are expressed as means±SEM (n=7 to 8); *$P<0.05$ vs euthyroid.

suggesting that the alterations were not attributable to a direct effect of thyroid hormone on vascular smooth muscle cells. Because physiological concentrations of thyroid hormones upregulated BMP4 in the contractile form of RAOSMCs and in vivo (hypothyroid versus euthyroid), BMP4 may be another direct target of thyroid hormone in aortic smooth muscle cells. However, the expected influences of the changes in all the calcification activators above were apparently masked, aforementioned, indicating their minor roles in vascular calcification, compared with those of calcification inhibitors.

In summary, our findings, for the first time, demonstrate that a physiological concentration of thyroid hormone has significant genomic effects on vascular smooth muscle cells in vitro and in vivo, which are associated with vascular calcification. Most notably, a decrease in thyroid hormone and the concomitant increase in vascular calcification in vivo are marked by a decrease in the level of MGP expression, suggesting that a physiological concentration of thyroid hormone has a direct protective role against vascular smooth muscle calcification in vivo. Although vascular calcification has been thought to be benign, arterial calcification should alter vascular compliance. Thus, it is possible that the increased vascular stiffness underlies the high systemic vascular resistance observed in hypothyroidism. Vascular calcification can lead to some other serious problems, including vascular stenosis, calciphylaxis, and even sudden death. Recently, a polymorphism in the promoter region of MGP gene was found to have a significant association with myocardial infarction in low-risk individuals and femoral calcification in the presence of atherosclerotic plaques, suggesting involvement of this mutation in coronary artery disease.[28] In addition, a recent meta-analysis of coronary artery calcium scores suggested that the calcium score is an independent risk factor to predict coronary heart disease events.[29] Therefore, further studies on the protective role of thyroid hormone and MGP against vascular smooth muscle calcification should provide insights into novel therapeutic strategies for the high systemic vascular resistance and blood pressure of hypothyroid patients, as well as for diseases associated with cardiovascular calcification such as diabetes, chronic renal insufficiency, and hypercholesterolemia.

Acknowledgments

This work was supported in part by grants from Japan Ministry of Health, Labor, and Welfare (H17-SAISEI-021), Japan Ministry of Education, Culture, Sports, Science, and Technology (13770052 and 15790141), the Japan Health Sciences Foundation (KH23106), and the Pharmaceuticals and Medical Devices Agency (MF-16).We thank Dr Youichi Shinozaki, Hidetoshi Tozaki, and Hiromi Yoshida for excellent technical assistance, and Dr Helen Kiriazis (Baker Heart Research Institute, Melbourne) for critical reading of this manuscript.

References

1. Carr AN, Kranias EG. Thyroid hormone regulation of calcium cycling proteins. *Thyroid.* 2002;12:453–457.
2. Abe A, Yamamoto T, Isome M, Ma M, Yaoita E, Kawasaki K, Kihara I, Aizawa Y. Thyroid hormone regulates expression of shaker-related potassium channel mRNA in rat heart. *Biochem Biophys Res Commun.* 1998;245:226–230.
3. Gloss B, Trost S, Bluhm W, Swanson E, Clark R, Winkfein R, Janzen K, Giles W, Chassande O, Samarut J, Dillmann W. Cardiac ion channel expression and contractile function in mice with deletion of thyroid hormone receptor alpha or beta. *Endocrinology.* 2001;142:544–550.
4. Boerth SR, Artman M. Thyroid hormone regulates Na^+-Ca^{2+} exchanger expression during postnatal maturation and in adult rabbit ventricular myocardium. *Cardiovasc Res.* 1996;31:E145–E152.
5. Orlowski J, Lingrel JB. Thyroid and glucocorticoid hormones regulate the expression of multiple Na,K-ATPase genes in cultured neonatal rat cardiac myocytes. *J Biol Chem.* 1990;265:3462–3470.
6. Klein I, Ojamaa K. Thyroid hormone and the cardiovascular system. *N Engl J Med.* 2001;344:501–509.
7. Ojamaa K, Klemperer JD, Klein I. Acute effects of thyroid hormone on vascular smooth muscle. *Thyroid.* 1996;6:505–512.
8. Hak AE, Pols HAP, Visser TJ, Drexhage HA, Hofman A, Witteman JC. Subclinical hypothyroidism is an independent risk factor for atherosclerosis and myocardial infarction in elderly women: the Rotterdam Study. *Ann Intern Med.* 2000;132:270–278.
9. Klein I, Ojamaa K. Thyroid hormone: targeting the vascular smooth muscle cell. *Circ Res.* 2001;88:260–261.
10. Mizuma H, Murakami M, Mori M. Thyroid hormone activation in human vascular smooth muscle cells: expression of type II iodothyronine deiodinase. *Circ Res.* 2001;88:313–318.
11. Fukuyama K, Ichiki T, Takeda K, Tokunou T, Iino N, Masuda S, Ishibashi M, Egashira K, Shimokawa H, Hirano K, Kanaide H, Takeshita A. Downregulation of vascular angiotensin II type 1 receptor by thyroid hormone. *Hypertension.* 2003;41:598–603.
12. Komar NN, Gabrielsen TO. Arterial calcification in adult cretins. *Am J Roentgenol Radium Ther Nucl Med.* 1967;101:202–203.
13. Tintut Y, Alfonso Z, Saini T, Radcliff K, Watson K, Bostrom K, Demer LL. Multilineage potential of cells from the artery wall. *Circulation.* 2003;108:2505–2510.

14. Bassett JH, Williams GR. The molecular actions of thyroid hormone in bone. *Trends Endocrinol Metab.* 2003;14:356–364.
15. Samuels HH, Stanley F, Casanova J. Depletion of L-3,5,3'-triiodothyronine and L-thyroxine in euthyroid calf serum for use in cell culture studies of the action of thyroid hormone. *Endocrinology.* 1979; 105:80–85.
16. Jono S, Nishizawa Y, Shioi A, Morii H. Parathyroid hormone-related peptide as a local regulator of vascular calcification. Its inhibitory action on in vitro calcification by bovine vascular smooth muscle cells. *Arterioscler Thromb Vasc Biol.* 1997;17:1135–1142.
17. Shioi A, Nishizawa Y, Jono S, Koyama H, Hosoi M, Morii H. Beta-glycerophosphate accelerates calcification in cultured bovine vascular smooth muscle cells. *Arterioscler Thromb Vasc Biol.* 1995;15: 2003–2009.
18. Sato Y, Ferguson DG, Sako H, Dorn GW II, Kadambi VJ, Yatani A, Hoit BD, Walsh RA, Kranias EG. Cardiac-specific overexpression of mouse cardiac calsequestrin is associated with depressed cardiovascular function and hypertrophy in transgenic mice. *J Biol Chem.* 1998;273:28470–28477.
19. Lazar MA, Chin WW. Nuclear thyroid hormone receptors. *J Clin Invest.* 1990;86:1777–1782.
20. Zebboudj AF, Shin V, Bostrom K. Matrix GLA protein and BMP-2 regulate osteoinduction in calcifying vascular cells. *J Cell Biochem.* 2003;90:756–765.
21. Shin V, Zebboudj AF, Bostrom K. Endothelial cells modulate osteogenesis in calcifying vascular cells. *J Vasc Res.* 2004;41:193–201.
22. Schug J, Overton GC. TESS: Transcription Element Search Software on the WWW. In: *Technical Report CBIL-TR-1997–1001-v0.0,* Computational Biology and Informatics Laboratory, School of Medicine, University of Pennsylvania, 1997:1–10.
23. Luo G, Ducy P, McKee MD, Pinero GJ, Loyer E, Behringer RR, Karsenty G. Spontaneous calcification of arteries and cartilage in mice lacking matrix GLA protein. *Nature.* 1997;386:78–81.
24. Vattikuti R, Towler DA. Osteogenic regulation of vascular calcification: an early perspective. *Am J Physiol Endocrinol Metab.* 2004;286: E686–E696.
25. Yoshiko Y, Maeda N, Aubin JE. Stanniocalcin 1 stimulates osteoblast differentiation in rat calvaria cell cultures. *Endocrinology.* 2003;144: 4134–4143.
26. Jono S, Peinado C, Giachelli CM. Phosphorylation of osteopontin is required for inhibition of vascular smooth muscle cell calcification. *J Biol Chem.* 2000;275:20197–20203.
27. Griethe W, Schmitt R, Jurgensen JS, Bachmann S, Eckardt KU, Schindler R. Bone morphogenic protein-4 expression in vascular lesions of calciphylaxis. *J Nephrol.* 2003;16:728–732.
28. Herrmann SM, Whatling C, Brand E, Nicaud V, Gariepy J, Simon A, Evans A, Ruidavets JB, Arveiler D, Luc G, Tiret L, Henney A, Cambien F. Polymorphisms of the human matrix gla protein (MGP) gene, vascular calcification, and myocardial infarction. *Arterioscler Thromb Vasc Biol.* 2000;20:2386–2393.
29. Pletcher MJ, Tice JA, Pignone M, Browner WS. Using the coronary artery calcium score to predict coronary heart disease events. A systematic review and meta-analysis. *Arch Intern Med.* 2004;164: 1285–1292.

THE JOURNAL OF BIOLOGICAL CHEMISTRY
© 2005 by The American Society for Biochemistry and Molecular Biology, Inc.

Vol. 280, No. 18, Issue of May 6, pp. 18434–18441, 2005
Printed in U.S.A.

$G\alpha_{12/13}$- and Reactive Oxygen Species-dependent Activation of c-Jun NH_2-terminal Kinase and p38 Mitogen-activated Protein Kinase by Angiotensin Receptor Stimulation in Rat Neonatal Cardiomyocytes*

Received for publication, August 24, 2004, and in revised form, February 28, 2005
Published, JBC Papers in Press, March 1, 2005, DOI 10.1074/jbc.M409710200

Motohiro Nishida‡§, Shihori Tanabe§¶, Yoshiko Maruyama¶, Supachoke Mangmool‡, Kyoji Urayama‡, Yuichi Nagamatsu‡, Shuichi Takagahara¶, Justin H. Turner‖, Tohru Kozasa, Hiroyuki Kobayashi‡, Yoji Sato‡‡, Toru Kawanishi‡‡, Ryuji Inoue§§, Taku Nagao‡‡, and Hitoshi Kurose‡¶¶**

*From the ‡Department of Pharmacology and Toxicology, Graduate School of Pharmaceutical Sciences, Kyushu University, 3-1-1 Maidashi, Higashi-ku, Fukuoka 812-8582, Japan, the ¶Laboratory of Cellular Signaling, Graduate School of Pharmaceutical Sciences, University of Tokyo, Tokyo 113-0033, Japan, the ‖Department of Medicine and Nephrology, Medical University of South Carolina, Charleston, South Carolina 29425, the **Department of Pharmacology, University of Illinois at Chicago, Chicago, Illinois 60612, the ‡‡National Institute of Health Sciences, Tokyo 158-8501, Japan, and the §§Department of Pharmacology, Graduate School of Medicine, Kyushu University, Fukuoka 812-8582, Japan*

In the present study, we examined signal transduction mechanism of reactive oxygen species (ROS) production and the role of ROS in angiotensin II-induced activation of mitogen-activated protein kinases (MAPKs) in rat neonatal cardiomyocytes. Among three MAPKs, c-Jun NH_2-terminal kinase (JNK) and p38 MAPK required ROS production for activation, as an NADPH oxidase inhibitor, diphenyleneiodonium, inhibited the activation. The angiotensin II-induced activation of JNK and p38 MAPK was also inhibited by the expression of the $G\alpha_{12/13}$-specific regulator of G protein signaling (RGS) domain, a specific inhibitor of $G\alpha_{12/13}$, but not by an RGS domain specific for $G\alpha_q$. Constitutively active $G\alpha_{12}$- or $G\alpha_{13}$-induced activation of JNK and p38 MAPK, but not extracellular signal-regulated kinase (ERK), was inhibited by diphenyleneiodonium. Angiotensin II receptor stimulation rapidly activated $G\alpha_{13}$, which was completely inhibited by the $G\alpha_{12/13}$-specific RGS domain. Furthermore, the $G\alpha_{12/13}$-specific but not the $G\alpha_q$-specific RGS domain inhibited angiotensin II-induced ROS production. Dominant negative Rac inhibited angiotensin II-stimulated ROS production, JNK activation, and p38 MAPK activation but did not affect ERK activation. Rac activation was mediated by Rho and Rho kinase, because Rac activation was inhibited by C3 toxin and a Rho kinase inhibitor, Y27632. Furthermore, angiotensin II-induced Rho activation was inhibited by $G\alpha_{12/13}$-specific RGS domain but not dominant negative Rac. An inhibitor of epidermal growth factor receptor kinase AG1478 did not affect angiotensin II-induced JNK activation cascade. These results suggest that $G\alpha_{12/13}$-mediated ROS production through Rho and Rac is essential for JNK and p38 MAPK activation.

Ang II[1] is a bioactive peptide involved in cardiac hypertrophy (1). Receptor stimulation by Ang II is assumed to activate G_q and G_i and turns on various signaling cascades dependent on cell types. Many groups have reported the regulation of MAPKs including JNK (2, 3), ERK (4, 5), and p38 MAPK (6) in a variety of cells (7). MAPKs are thought to be key intracellular transducers of mitogenic stimulation and have been implicated in the signaling pathways leading to cardiac hypertrophy (8, 9). An earlier study demonstrated that Ang II-induced JNK activation is dependent on extracellular calcium and protein kinase C and partially on a tyrosine kinase (2). On the other hand, Ang II-induced ERK activation is mediated by the Ras pathway or protein kinase C pathway (10). A recent study showed that β-arrestin-mediated internalization of ATR is involved in ERK activation (11). ERK or p38 MAPK activation by Ang II requires the EGF receptor transactivation, whereas JNK activation is regulated by other signaling proteins (7). These results indicate that the signal transduction mechanism of MAPK activation depends on the types of MAPKs and cellular contexts that are analyzed.

ROS such as hydrogen peroxide and oxygen radicals play various roles in living cells as a second messenger to elicit physiological responses or as a toxic intermediate leading to cellular damage (12). Recent studies suggest that ROS work as regulators of signal transduction (13, 14). We have reported that heterotrimeric $G_{i/o}$ proteins are putative target molecules of ROS (15, 16). Although Ang II produces ROS in vascular smooth muscle cells and cardiac myocytes (6, 17, 18), the molecular mechanism of ROS production and the identification of ROS target molecules are largely unknown.

Rac, one of the small GTP-binding proteins, is believed to participate in the production of ROS by activating NADPH oxidase in neutrophil (19). Previous findings have demonstrated that one of the Rac effector PAKs mediates JNK activation by Ang II, and PAK phosphorylates a subunit of the NADPH oxidase complex (20). MAPKs are activated by Rac as

* This work was supported in part by a grant (to M. N., T. N, and H. K.) from the Ministry of Education, Science, Sports, and Culture of Japan. The costs of publication of this article were defrayed in part by the payment of page charges. This article must therefore be hereby marked "*advertisement*" in accordance with 18 U.S.C. Section 1734 solely to indicate this fact.

§ These authors contributed equally to this work.

¶¶ To whom correspondence should be addressed. Tel. and Fax: 81-92-642-6884; E-mail: kurose@phar.kyushu-u.ac.jp.

[1] The abbreviations used are: Ang II, angiotensin II; ATR, angiotensin receptor; AT1R, angiotensin type 1 receptor; CA, constitutively active; DCF, 2′,7′-dichlorofluorescein diacetate; DPI, diphenyleneiodonium; DN, dominant negative; EGF, epidermal growth factor; ERK, extracellular signal-regulated kinase; GRK2, G protein-coupled receptor kinase 2; GST, glutathione *S*-transferase; GST-TPR, GST fusion protein with TPR domain of protein phosphatase 5; JNK, c-Jun NH_2-terminal kinase; MAPK, mitogen-activated protein kinase; MOI, multiplicity of infection; PAK, p21-activated kinase; Prx, peroxiredoxin; PTX, pertussis toxin; RGS, regulator of G protein signaling; ROCK, Rho-associated kinase; ROS, reactive oxygen species; TPR, tetratricopeptide repeat.

well as RhoA and Raf-1, and the resulting activation of MAPKs induces hypertrophic responses through the activation of intracellular signaling cascades (21–24). However, upstream molecules of and the relationship between these intracellular signaling molecules are not fully determined.

G_{12} family G proteins, G_{12} and G_{13}, couple with various G protein-coupled receptors and mediate physiological responses by interacting with different signaling proteins (25). The role of $G_{12/13}$ in the heart, however, has not been revealed because of the unavailability of a specific inhibitor. Recent studies showed that p115RhoGEF has an RGS domain for $G\alpha_{12/13}$ (26, 27). We examined by using the RGS domain of p115RhoGEF whether $G_{12/13}$ is involved in Ang II-mediated signal transduction pathway and ROS production and whether ROS work as a mediator in cardiac myocytes. To demonstrate the signal transduction cascade, we constructed various recombinant adenoviruses coding $G\alpha_{12/13}$- or $G\alpha_q$-specific RGS domains and DN-Rac. We demonstrate in the present study that Ang II-induced JNK and p38 MAPK activation requires ROS, and Ang II-induced ROS production is mediated by sequential activation of $G_{12/13}$, Rho, and Rac.

EXPERIMENTAL PROCEDURES

Materials and Plasmid Construction—AT1R blocker CV11974 was provided from Takeda Chemical Industries Ltd. (Osaka, Japan). AG1478, PTX, and Y27632 were purchased from Calbiochem. DPI, *N*-acetyl-L-cysteine, catalase, and PD123319 were from Sigma. Fura-2/AM was from Dojindo (Kumamoto, Japan). Collagenase and FuGENE 6 were from Roche Applied Science. 2′,7′-Dichlorofluorescein diacetate was from Molecular Probe. Glutathione-Sepharose beads were from Amersham Biosciences. The cDNA coding DN-Rac1 was provided by Dr. Kozo Kaibuchi (Nagoya University, Nagoya, Japan). The plasmid coding PrxII was provided by Dr. Sue Goo Rhee (National Institutes of Health). The sequence coding Cdc42/Rac interactive binding domain of PAK was cloned from mouse brain, sequenced, and ligated into pGEX-4T-1 to make GST fusion protein construct. GST-TPR construct was provided by Dr. Manabu Negishi (Kyoto University, Kyoto, Japan). GST fusion proteins were expressed at room temperature and purified using glutathione-Sepharose as described (28, 29). Rat AT1R was cloned from rat heart, and the sequence was confirmed. Anti-phospho-ERK and anti-ERK antibodies were purchased from Cell Signaling. Anti-phospho-p38 MAPK and anti-p38 MAPK antibodies were from Promega. Anti-$G\alpha_{13}$, anti-RhoA, horseradish peroxidase-conjugated anti-rabbit IgG, and anti-mouse IgG antibodies were from Santa Cruz Biotechnology. Anti-Rac1 antibody was from Transduction Laboratories.

Production of Adenoviruses—Recombinant adenoviruses of DN-Rac, PrxII, p115-RGS (the RGS domain of p115RhoGEF), GRK2-RGS, C3 toxin, CA-$G\alpha_q$ (R183C), CA-$G\alpha_{12}$ (Q229L), and CA-$G\alpha_{13}$ (Q226L) were produced by the method of He *et al.* (30) with a slight modification. Recombinant adenoviruses that do not express green fluorescent protein were also produced for DN-Rac, PrxII, hemagglutinin-tagged p115-RGS, and hemagglutinin-tagged GRK2-RGS. Adenovirus expressing GRK2-ct (the carboxyl-terminal domain of GRK2 that sequesters $\beta\gamma$ subunits) was produced by the method as described (31). Adenovirus of LacZ was obtained from the RIKEN DNA Bank (Tsukuba, Japan).

Determination of JNK, ERK, and p38 MAPK Activation—The rat neonatal cardiac myocytes were isolated from 1–2-day-old Sprague-Dawley rat pups as previously described (15). The activity of JNK was determined as described (32, 33). ERK and p38 MAPK activation were determined by Western blot analysis using phospho-specific antibodies (32, 33). The optical density of the film was scanned and measured with Scion Image Software.

Quantification of Intracellular ROS Produced by Ang II Receptor Stimulation—ROS production was measured with the fluorescent dye DCF as described (34). The cardiomyocytes were plated on glass-bottomed 35-mm dishes and incubated for 10 min with 5 μM DCF. The DCF fluorescence at an emission wavelength of 510 nm was observed at room temperature by exciting DCF at 488 nm using a video image analysis system (Aquacosmos, Hamamatsu Photonics).

Measurement of Rac Activity—Activation of Rac was measured by the method of Ren and Schwartz (35) with a slight modification. Forty-eight h after adenovirus infection, the cardiomyocytes were stimulated by Ang II and lysed in buffer containing 50 mM Tris (pH 7.2), 1% Triton X-100, 0.5% sodium deoxycholate, 0.1% SDS, 500 mM NaCl, 10 mM $MgCl_2$, 10 μg/ml leupeptin, 10 μg/ml aprotinin, 1 mM phenylmethylsulfonyl fluoride, and 4 μg of GST-PAK-Cdc42/Rac interactive binding domain. Supernatant was incubated with glutathione-Sepharose beads for 2 h at 4 °C. The beads were washed and finally suspended in SDS sample buffer. Pulled down Rac was detected with anti-Rac1 antibody.

Measurement of Rho Activity—Rho activation was determined by the method of Maruyama *et al.* (32). Cells were stimulated by Ang II (100 nM) for 1 min, and lysed in buffer containing 50 mM Tris (pH 7.5), 0.1% Triton X-100, 10% glycerol, 150 mM NaCl, 30 mM $MgCl_2$, 1 mM dithiothreitol, 10 μg/ml leupeptin, 10 μg/ml aprotinin, 1 mM phenylmethylsulfonyl fluoride. The supernatant of cell lysates was incubated with 12 μg of GST-Rho-binding domain and glutathione-Sepharose beads for 120 min at 4 °C. The bead was washed, and finally suspended in SDS sample buffer. Pulled down Rho was detected with anti-Rho antibody.

Measurement of $G\alpha_{13}$ Activity—HEK293 cells in six-well dishes were transfected with rat wild type AT1R and $G\alpha_{13}$ with or without respective RGS domains, using FuGENE 6 reagent. Cardiomyocytes in 60-mm dishes were infected with LacZ, p115-RGS, or GRK2-RGS at 100 MOI or with CA-$G\alpha_{13}$ at 30 MOI. Forty-eight h after transfection, activation of $G\alpha_{13}$ was measured by the method of Yamaguchi *et al.* (36). After Ang II stimulation, the cells were harvested with 500 μl of ice-cold lysis buffer containing 20 mM Hepes (pH 8.0), 2 mM $MgCl_2$, 1 mM EDTA, 1 mM dithiothreitol, 0.5% Triton X-100, 1 mM phenylmethylsulfonyl fluoride, 10 μg/ml aprotinin, 10 μg/ml leupeptin, and 10 μg of GST-TPR. The cell lysates were then centrifuged for 5 min at 12,000 × *g*, and the supernatants were incubated with glutathione-Sepharose bead for 120 min at 4 °C. The bead was washed and finally suspended in SDS sample buffer. Pulled down $G\alpha_{13}$ was detected with anti-$G\alpha_{13}$ antibody.

Intracellular Ca^{2+} Measurement—The intracellular Ca^{2+} concentration ($[Ca^{2+}]_i$) of cardiomyocytes was determined as described previously (21, 33). Briefly, the cells (1×10^6) were plated on gelatin-coated glass-bottomed 35-mm dishes and were loaded with 2.5 μM Fura-2/AM in the cultured medium at 37 °C for 30 min. The cells were washed with Tyrode solution containing 118 mM NaCl, 5.4 mM KCl, 2 mM $CaCl_2$, 2 mM $MgCl_2$, 10 mM Hepes (pH 7.4), 0.33 mM NaH_2PO_4, 10 mM glucose, and 30 mM taurine. Fluorescence images of green fluorescent protein-positive cells were recorded and analyzed with a video image analysis system (Aquacosmos, Hamamatsu Photonics). All of the ratio data were calculated for determination of $[Ca^{2+}]_i$ with *in vivo* calibration method.

Statistical Analysis—The results are shown as the means ± S.E. The mean values were compared with control by Student's *t* test (for two groups) or one-way analysis of variance followed by Dunnett's test (for three or more groups).

RESULTS

Ang II-induced MAPK Activation—To delineate the signal transduction cascade leading to MAPK activation by Ang II stimulation, the concentration dependence and time course of MAPK activation were determined. Stimulation with Ang II resulted in a dose-dependent activation of ERK, JNK, and p38 MAPK (Fig. 1*A*). The EC_{50} values of Ang II to activate ERK, JNK, or p38 MAPK were different between three MAPKs. ERK, JNK, and p38 MAPK activation peaked at 5, 20, and 20 min, respectively (Fig. 1*B*). These results demonstrate that Ang II stimulation activated three MAPKs in cardiac myocytes.

ROS Mediate Ang II-induced JNK and p38 MAPK Activation—We examined first which MAPK requires ROS for their activation. One of ROS producing systems is NADPH oxidase complex, which is activated by receptor stimulation. Thus, we examined the effects of chemical antioxidants, such as *N*-acetyl-L-cysteine (a radical scavenger), DPI (an NADPH oxidase inhibitor), and catalase (an H_2O_2-degrading enzyme), on MAPK activation. Ang II-induced ERK activation was not affected by these antioxidants (Fig. 1*C*). However, Ang II-induced activation of p38 MAPK and JNK was inhibited by all three reagents (Fig. 1, *D* and *E*). We have also found that the expression of Prx II (a radical scavenging enzyme) significantly inhibited Ang II-induced JNK activation but not ERK activation (data not shown). These results indicate that JNK and p38 MAPK activation are sensitive to ROS and suggest that ROS produced by NADPH oxidase is necessary for Ang II-induced JNK and p38 MAPK activation.

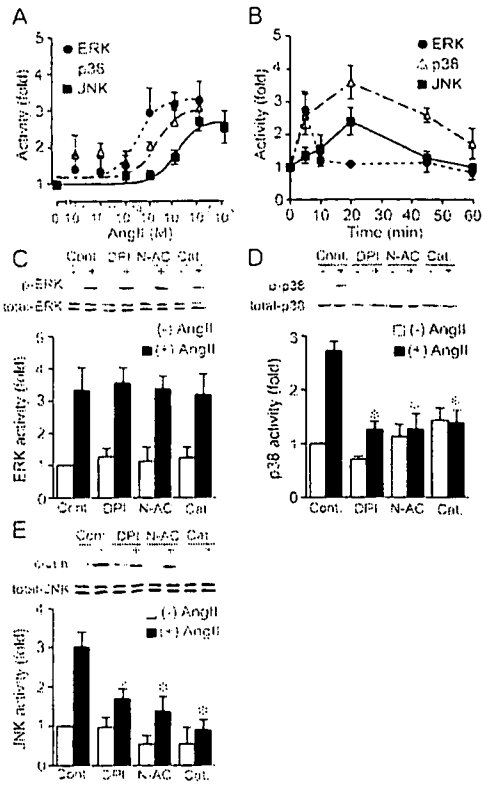

FIG. 1. **ROS-dependent activation of JNK and p38 MAPK by ATR stimulation.** *A*, dose-dependent activation of JNK, ERK, or p38 MAPK by Ang II stimulation. JNK, ERK, or p38 MAPK (p38) activities were measured at 20, 5, and 10 min after Ang II stimulation with the indicated concentrations. *B*, time course of JNK, ERK, or p38 MAPK activation. Ang II (100 nM) stimulation activated JNK and increased the phosphorylation of p38 MAPK, which peaked at 20 min. Ang II (10 nM) increased the phosphorylation of ERK, which peaked at 5 min. *C–E*, effects of DPI, *N*-acetyl-L-cysteine (*N-AC*) or catalase (*Cat.*) on Ang II-induced ERK (*C*), p38 MAPK (*D*), JNK (*E*) activation. Before the addition of Ang II, the cells were treated with DPI (5 μM), *N*-acetyl-L-cysteine (300 μM), or catalase (100 units/ml) for 20, 30, or 30 min, respectively. The results are shown as the means ± S.E. from three to five experiments. *, $p < 0.05$ *versus* Ang II stimulation of control (*Cont.*) cells.

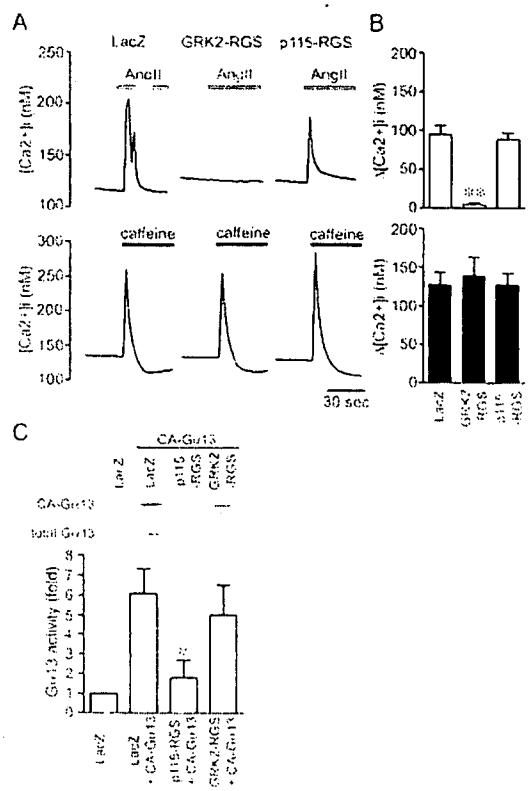

FIG. 2. **Selectivity of GRK2-RGS and p115-RGS in neonatal cardiac myocytes as determined by Ang II-induced Ca^{2+} release.** *A*, effects of GRK2-RGS and p115-RGS on Ang II-stimulated increases in $[Ca^{2+}]_i$. The cells were infected by adenovirus encoding LacZ (100 MOI), p115-RGS (100 MOI), or GRK2-RGS (300 MOI). Forty-eight h after infection, the cells were stimulated with 100 nM Ang II (*upper panel*) or 10 mM caffeine (*lower panel*) in Ca^{2+}-free EGTA-containing Tyrode solution. *B*, Ang II- or caffeine-induced increases in $[Ca^{2+}]_i$ were calculated and plotted. $[Ca^{2+}]_i$ was monitored from 9–22 cells, and the average trace of $[Ca^{2+}]_i$ was calculated and plotted. The experiment was repeated three times. **, $p < 0.01$ *versus* Ang II stimulation of LacZ-expressing cells. *C*, selectivity of p115-RGS in neonatal cardiac myocytes was determined by pull-down assay. Pull-down assay was performed by pull-down of active form of $G\alpha_{13}$ using GST-TPR. The cells were co-infected with adenoviruses encoding LacZ and CA-$G\alpha_{13}$, p115-RGS and CA-$G\alpha_{13}$, or GRK2-RGS and CA-$G\alpha_{13}$ at 50 MOI, respectively. The cell lysates were incubated with GST-TPR, and the bound $G\alpha_{13}$ was detected by immunoblotting with anti-$G\alpha_{13}$ antibody. *, $p < 0.05$ *versus* LacZ and CA-$G\alpha_{13}$-expressing cells. The experiment was repeated three times.

Selective Inhibition of $G\alpha_{12/13}$ by the Expression of p115-RGS—To investigate which G protein is involved in Ang II-induced MAPK activation, a variety of adenoviruses that specifically inhibit G protein-mediated signaling were produced. Among them, p115-RGS or GRK2-RGS was used to specifically inhibit $G\alpha_{12/13}$ or $G\alpha_q$, respectively. To delineate the selectivity of GRK2-RGS and p115-RGS, two RGS domains were expressed, and Ang II-stimulated increase in $[Ca^{2+}]_i$ was determined in the absence of extracellular Ca^{2+}. Ang II stimulation increased $[Ca^{2+}]_i$ (Fig. 2). Because $[Ca^{2+}]_i$ was measured in the absence of extracellular Ca^{2+}, the increase in $[Ca^{2+}]_i$ represents the activation of $G\alpha_q$-phospholipase C pathway. GRK2-RGS completely blocked the increase in $[Ca^{2+}]_i$, but p115-RGS did not (Fig. 2, *A* and *B*). GRK2-RGS did not affect the caffeine-induced increase in $[Ca^{2+}]_i$. Because caffeine promotes Ca^{2+} release from intracellular Ca^{2+} pool, the effect of GRK2-RGS is specific for the receptor-stimulated increase in $[Ca^{2+}]_i$. These results suggest that GRK2-RGS but not p115-RGS blocks ATR-mediated phospholipase C activation through $G\alpha_q$. We have also examined the specificity of p115-RGS. Because signaling molecule downstream of $G\alpha_{12/13}$ such as $[Ca^{2+}]_i$ and cAMP has not been firmly established, we directly measured the activation of $G\alpha_{12/13}$ by Ang II stimulation. It has been reported that $G\alpha_{12/13}$ activation can be detected by selective pull-down of activated $G\alpha_{12/13}$ using the TPR domain of protein phosphatase type 5 (36). Then we examined whether p115-RGS selectively inhibits Ang II receptor-stimulated $G\alpha_{12/13}$ activation by pull-down assay, using CA-$G\alpha_{13}$ as a positive control. Expression of CA-$G\alpha_{13}$ increased the amount of CA-$G\alpha_{13}$ pulled down by GST-TPR (Fig. 2*C*). The amount of pulled down $G\alpha_{13}$ was completely abolished by p115-RGS, but not by GRK2-RGS. Because p115-RGS encodes RGS domain specific for $G\alpha_{12/13}$ and the RGS domain can bind $G\alpha$ in active conformation, the mechanism of this inhibition by p115-RGS is competition between p115-RGS and GST-TPR for the binding of CA-$G\alpha_{13}$. By considering that p115-RGS did not affect the Ang II-induced increase in $[Ca^{2+}]_i$, it is concluded that p115-RGS specifically binds the active form of $G\alpha_{13}$.

Activation of $G_{12/13}$ by ATR Stimulation—In AT1R- and $G\alpha_{13}$-expressing HEK293 cells, AT1R stimulation rapidly activated $G\alpha_{13}$ (Fig. 3*A*). The activation reached a maximum at 3 min and sustained more than 2-fold for about 10 min. The Ang II-induced $G\alpha_{13}$ activation was completely inhibited by p115-RGS, but not by GRK2-RGS (Fig. 3*B*). Because the RGS domain

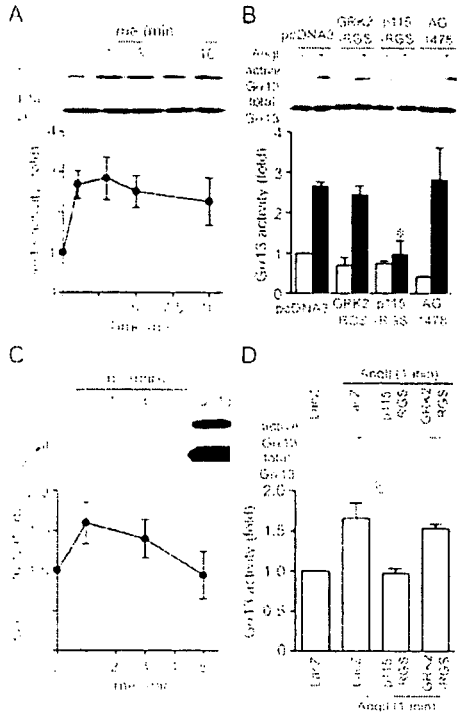

FIG. 3. **Activation of $G\alpha_{13}$ by AT1R stimulation in HEK293 cells and cardiac myocytes.** Selectivity of p115-RGS in HEK293 cells was determined by pull-down assay. *A*, time-dependent activation of $G\alpha_{13}$ by AT1R stimulation in wild type AT1R- and $G\alpha_{13}$-expressing HEK293 cells. The cell lysates were incubated with GST-TPR, and bound $G\alpha_{13}$ was detected by immunoblotting with anti-$G\alpha_{13}$ antibody. *B*, effects of p115-RGS, GRK2-RGS or AG1478 on Ang II-stimulated activation of $G\alpha_{13}$. HEK293 cells were transfected with p115-RGS or GRK2-RGS, with AT1R and $G\alpha_{13}$. The cells were treated with AG1478 (500 nM) for 20 min before the addition of Ang II (100 nM, 3 min). The experiments were repeated five times. *, $p < 0.05$ *versus* Ang II stimulation of pcDNA3-transfected cells. *C*, time-dependent activation of $G\alpha_{13}$ by ATR stimulation in neonatal cardiac myocytes. The cardiac myocytes were stimulated with Ang II (100 nM) for the indicated times. For positive control, the cells were infected with CA-$G\alpha_{13}$ (30 MOI). *D*, effect of p115-RGS or GRK2-RGS on Ang II-induced activation of $G\alpha_{13}$ in cardiac myocytes. The cells were stimulated with Ang II (100 nM) for 1 min. The experiments were repeated five to six times. *, $p < 0.05$, as statistically analyzed by Student's *t* test.

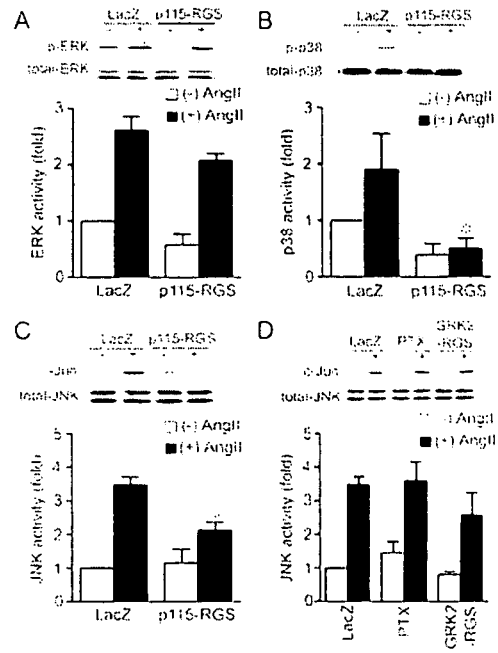

FIG. 4. **Effects of p115-RGS on Ang II-stimulated MAPK activation.** Cardiac myocytes were infected with LacZ- or p115-RGS-expressing adenoviruses. The cells were stimulated with Ang II (100 nM) for 20 min (JNK and p38 MAPK) or with 10 nM for 5 min (ERK), and ERK phosphorylation (*A*), p38 MAPK phosphorylation (*B*), or JNK activity (*C*) were determined. *D*, cells were infected by adenovirus encoding LacZ (100 MOI) or GRK2-RGS (300 MOI). Some portion of cells was treated with PTX (100 ng/ml) for 24 h before the addition of Ang II. The fold activation was calculated by the values of untreated cells infected with LacZ set as 1. *, $p < 0.05$ *versus* Ang II stimulation of LacZ-expressing cells. The experiments were repeated three to ten times.

of p115-RGS has the ability to accelerate GTPase activity of $G\alpha_{12/13}$, the mechanism of this inhibition by p115-RGS is the inactivation of GTP-bound $G\alpha_{13}$. Fig. 3*B* also shows that AG1478 treatment did not inhibit Ang II-stimulated $G\alpha_{13}$ activation (Fig. 3*B*). This result suggests that the EGF receptor is not involved in AT1R-mediated $G\alpha_{13}$ activation. Furthermore, stimulation of endogenous ATR also activated $G\alpha_{13}$ in rat cardiac myocytes (Fig. 3*C*). The activation reached a maximum at 1 min and gradually decreased to the basal level within 5 min. This Ang II-induced $G\alpha_{13}$ activation was completely inhibited by p115-RGS but not by GRK2-RGS (Fig. 3*D*). These results indicate that stimulation of AT1R activates not only G_q but also G_{13} and that p115-RGS selectively inhibits Ang II-induced $G\alpha_{13}$ activation.

$G_{12/13}$ Mediates Ang II-induced JNK and p38 MAPK Activation—We examined whether $G\alpha_{12/13}$ is involved in Ang II-induced MAPK activation. Ang II-induced ERK activation was not affected by p115-RGS, but the activation of JNK and p38 MAPK was significantly inhibited by p115-RGS (Fig. 4, *A–C*). We also used PTX to block ATR-G_i coupling. PTX treatment and expression of GRK2-RGS did not affect Ang II-induced JNK activation (Fig. 4*D*). We also confirmed that Ang II-induced p38 MAPK activation was insensitive to PTX or GRK2-RGS ($n = 2$; data not shown). These results suggest that the activation of JNK and p38 MAPK is mainly mediated by $G\alpha_{12/13}$ but not $G\alpha_q$ and G_i. These results indicate that ATR couples with $G_{12/13}$, and $G\alpha_{12/13}$ activates signal transduction cascade, leading to JNK and p38 MAPK activation.

ROS-dependent Activation of JNK and p38 MAPK Induced by $G\alpha_{12/13}$ Activation—We next determined the relationship between $G\alpha_{12/13}$ and ROS in Ang II-induced JNK and p38 MAPK activation. Expression of CA-$G\alpha_q$, CA-$G\alpha_{12}$, or CA-$G\alpha_{13}$ resulted in activation of all three MAPKs (Fig. 5). This result indicates that activated $G\alpha_q$, $G\alpha_{12}$, or $G\alpha_{13}$ can induce activation of MAPKs in neonatal cardiac myocytes. Furthermore, $G\alpha_{12}$- or $G\alpha_{13}$-induced activation of p38 MAPK (Fig. 5*B*) and JNK (Fig. 5*C*), but not ERK (Fig. 5*A*), was sensitive to DPI. In contrast, $G\alpha_q$-induced JNK and p38 MAPK activation was not affected by DPI. These results are consistent with the fact that activation of $G\alpha_{12/13}$ by ATR stimulation activates JNK and p38 MAPK through ROS production.

Rac-dependent ROS Production by ATR Stimulation—We examined whether ATR stimulation actually produces ROS in rat neonatal cardiomyocytes. Fig. 6*A* shows that exposure of Ang II increased intracellular concentration of ROS. The concentration of ROS by Ang II stimulation was compared with the amount of fluorescence generated by exogenously added H_2O_2. Ang II stimulation increased ROS to about 4 μM, and p115-RGS and PrxII inhibited ROS production (Fig. 6*B*). However, the Ang II-induced ROS production was not affected by GRK2-RGS. These results indicate that $G\alpha_{12/13}$ but not $G\alpha_q$ mediates Ang II-induced ROS production. Furthermore, expression of DN-Rac or treatment with DPI inhibited Ang II-induced ROS production, suggesting that NADPH oxidase mediates Ang II-induced ROS production.

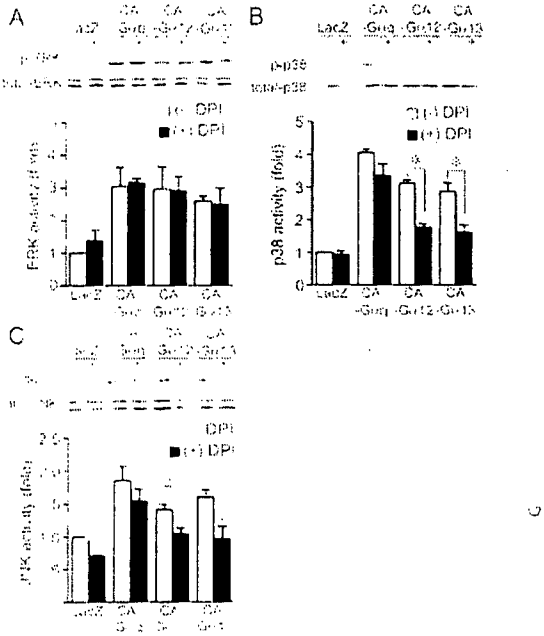

FIG. 5. **ROS-dependent JNK and p38 MAPK activation or ROS-independent ERK activation following the expression of CA-$G\alpha_q$, CA-$G\alpha_{12}$, or CA-$G\alpha_{13}$.** The cells were infected by adenovirus encoding LacZ (100 MOI), CA-$G\alpha_q$ (100 MOI), CA-$G\alpha_{12}$ (100 MOI), or CA-$G\alpha_{13}$ (30 MOI). Forty-eight h after infection, the cells were treated with DPI (5 μM) for 30 min, and then ERK (*A*), p38 MAPK phosphorylation (*B*), and JNK activity (*C*) were determined. *, $p < 0.05$ *versus* MAPK activation without DPI of LacZ-, CA-$G\alpha_{12}$-, or $G\alpha_{13}$-expressing cells. The experiments were repeated three times.

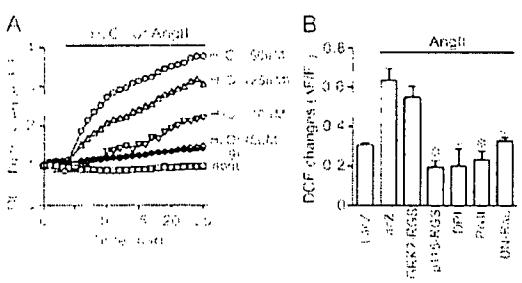

FIG. 6. **Inhibition of Ang II-induced ROS production by p115-RGS and DN-Rac.** *A*, average changes in H_2O_2- or Ang II-induced F/F_o of DCF from time course experiments. The cells were stimulated by the indicated concentration of H_2O_2 or by Ang II (100 nM). The *traces* are shown as averages from 22–36 cells. *B*, the increase in Ang II-induced florescence of DCF was calculated by the value of maximal fluorescence intensity during 25 min of stimulation and the initial value of fluorescence, F_o. The cells were treated with DPI (5 μM) for 20 min prior to Ang II stimulation. Ang II-stimulated DCF fluorescence was also determined in cells expressing GRK2-RGS, p115-RGS, PrxII, or DN-Rac. *, $p < 0.05$ *versus* Ang II stimulation of LacZ-expressing cells. The experiments were repeated three times.

$G\alpha_{12/13}$ Activates Rac Leading to JNK and p38 MAPK Activation—We examined the involvement of Rac in Ang II-induced MAPK activation. Expression of DN-Rac inhibited Ang II-induced activation of JNK and p38 MAPK, but not ERK (Fig. 7, *A–C*). Because DN-Rac inhibited Ang II-induced ROS production (Fig. 6*B*), Rac may mediate Ang II-induced JNK and p38 MAPK activation through ROS production. Rac activation can be determined by selective pull-down assay using the Cdc42/Rac interactive binding domain of PAK that is one of the Rac effectors. Rac activation was detected by angiotensin II stimulation, which peaked at 1 min and quickly returned to the basal state (data not shown). As expected, the expression of DN-Rac

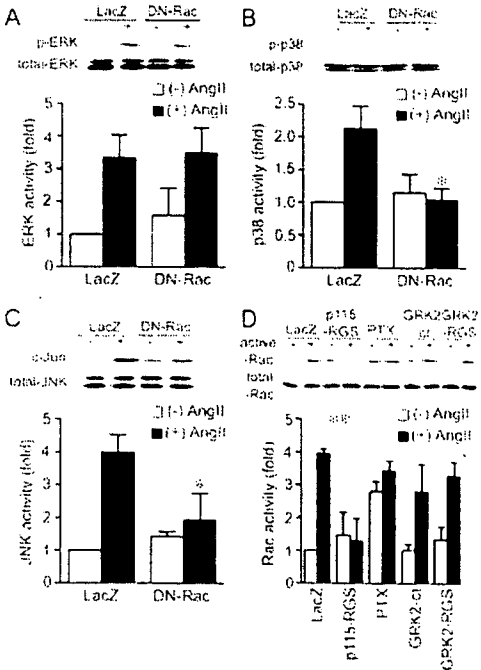

FIG. 7. **Effects of DN-Rac on Ang II-stimulated MAPK activation.** Cardiac myocytes were infected with adenovirus encoding LacZ or DN-Rac. *A–C*, cells were stimulated with Ang II (100 nM) for 20 min (JNK and p38 MAPK) or with 10 nM for 5 min (for ERK). The activation of ERK (*A*), p38 MAPK (*B*), and JNK (*C*) were then determined. *, $p < 0.05$ *versus* Ang II stimulation of LacZ-expressing cells. *D*, cardiac myocytes were infected with p115-RGS or GRK2-ct at 100 MOI or were infected with GRK2-RGS at 300 MOI. Some portion of cells were treated with PTX (100 ng/ml) for 24 h before the addition of Ang II. Rac activation was determined by pull-down assay. The fold activation was calculated by the values of untreated cells infected with LacZ set as 1. *, $p < 0.01$ *versus* Ang II stimulation of LacZ-expressing cells. The experiments were repeated three to four times.

completely inhibited Ang II-induced activation of JNK and p38 MAPK but not ERK (Fig. 7, *A–C*). Rac activation was inhibited by p115-RGS, but not by PTX, GRK2-ct (a G$\beta\gamma$-sequestering polypeptide), and GRK2-RGS (Fig. 7*D*). The basal Rac activity of PTX-treated cells was increased for unknown reasons. Similar high basal Rac binding activity with PTX treatment has been reported by another group (37). These results suggest that $G_{12/13}$ mediate Ang II-induced Rac activation.

Rho Mediates Ang II-induced Rac Activation—Because p115-RGS inhibited JNK, p38 MAPK, and Rac activation, we speculated that $G\alpha_{12/13}$ may activate JNK, p38 MAPK, and Rac through Rho activation. Rho is specifically inactivated by C3 toxin that ADP-ribosylates Asn at position 41 of Rho. The expression of C3 toxin inhibited Ang II-stimulated JNK and Rac activation (Fig. 8, *A* and *B*). These results indicate that Rho mediates Rac and JNK activation by ATR stimulation. Because Rho regulates various kinases including ROCK, we next examined whether ROCK mediates Ang II-induced Rac activation (38). A ROCK inhibitor, Y27632, inhibited Rac activation (Fig. 8*C*). These results suggest that Ang II-induced Rac activation is mediated by Rho and consequent activation of ROCK. Furthermore, stimulation of ATR with Ang II activated Rho by 3-fold, which was completely inhibited by p115-RGS, but not GRK2-RGS and DN-Rac (Fig. 8*D*). Because ROS production is inhibited by DN-Rac, Ang II-induced Rho/ROCK activation could participate in Rac-dependent ROS production. These results also suggest that Rac activation is downstream of Rho activation.

ATR Subtype and Role of EGF Receptor Transactivation for Ang II-induced JNK Activation—Ang II-induced JNK activa-

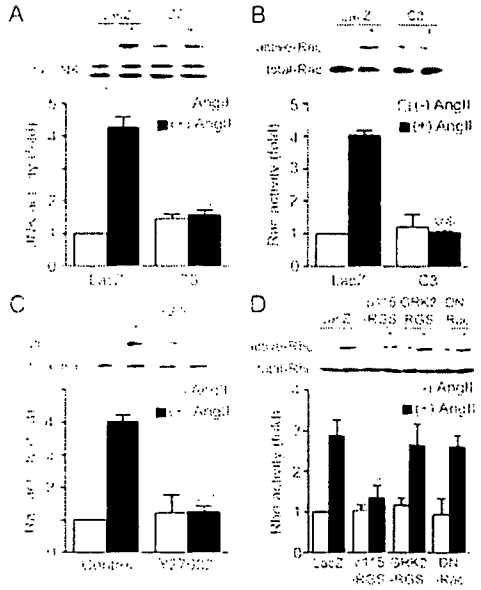

FIG. 8. **Rho-mediated activation of JNK and Rac.** Cardiac myocytes were infected with adenovirus expressing C3 toxin. The cells were then stimulated with Ang II (100 nM) for 20 min (JNK activation) or 1 min (Rac activation), and JNK activity (*A*) and Rac activation (*B*) were determined. *C*, cardiac myocytes were treated with a ROCK inhibitor Y27632 (10 μM) for 30 min. The cells were then stimulated with Ang II (100 nM) for 1 min, and Rac activation was determined. The fold activation was calculated by the values of untreated cells infecting with LacZ set as 1. **, $p < 0.01$ *versus* Ang II stimulation of control (LacZ-expressing) cells. *D*, cells were infected with adenovirus encoding p115-RGS, GRK2-RGS, or DN-Rac. The cells were then stimulated with Ang II (100 nM) for 1 min, and Rho activation was determined. *, $p < 0.05$ *versus* Ang II stimulation of LacZ-expressing cells. The experiments were repeated three to four times.

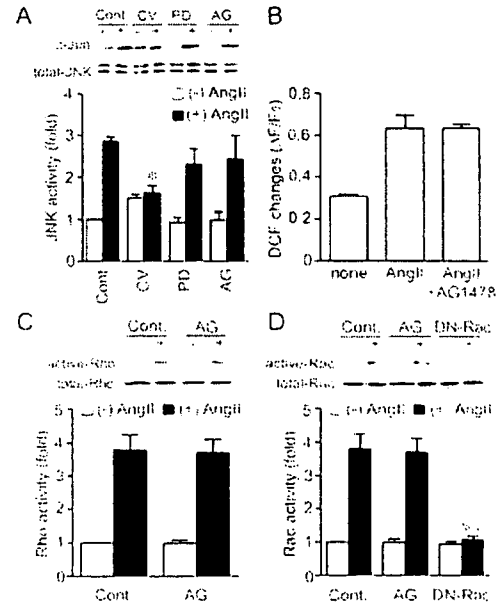

FIG. 9. **Effects of Ang II receptor subtype selective blockers or EGF receptor kinase inhibitor on Ang II-induced JNK activation cascade.** *A*, cells were treated with CV11974 (*CV*, 1 μM), PD123319 (*PD*, 5 μM), or AG1478 (*AG*, 500 nM) for 20 min before the addition of Ang II (100 nM, 20 min), and JNK activation was determined. *, $p < 0.05$ *versus* Ang II stimulation of control cells (*Cont.*). *B*, effect of an EGF receptor kinase inhibitor AG1478 on Ang II-induced ROS production. The cells were treated with AG1478 (500 nM) for 20 min before the addition of Ang II (100 nM, 25 min), and ROS production was measured. *C*, effect of AG1478 on Ang II-induced Rho activation. The cells were stimulated with Ang II (100 nM) for 1 min, and Rho activation was determined by pull-down assay. The fold activation was calculated by the values of untreated cells (control) set as 1. *D*, effect of AG1478 or DN-Rac on Ang II-induced Rac activation. The cells were infected with DN-Rac at 300 MOI or treated with AG1478 (500 nM, 20 min), and Rac activation was determined by pull-down assay. **, $p < 0.01$ *versus* Ang II stimulation of control cells. The experiments were repeated three times.

tion was significantly inhibited by CV11974 (a selective AT1R blocker), but not by PD123319 (a selective AT2R blocker), indicating that JNK was activated by type 1 subtype of ATR (Fig. 9*A*). It has been reported that EGF receptor transactivation plays an important role in G protein-coupled receptor-induced MAPK activation including AT1R (7). To examine the involvement of EGF receptor transactivation, we used an inhibitor of EGF receptor kinase AG1478. AG1478 did not affect Ang II-stimulated $G\alpha_{13}$ activation (Fig. 3*B*), JNK activation, ROS production, Rho activation, and Rac activation (Fig. 9). DN-Rac inhibited Rac activation, validating the assay method (Fig. 9*D*). These results suggest that EGF receptor is not involved in Ang II-induced JNK activation through $G\alpha_{12/13}$-mediated Rho/ROCK activation in cardiac myocytes.

DISCUSSION

We demonstrated in the present study that Ang II-induced JNK/p38 MAPK activation was mediated by a ROS-dependent signal transduction pathway: Ang II → AT1R → $G\alpha_{12/13}$ → Rho → ROCK → Rac → ROS → JNK/p38 MAPK (Fig. 10). We clearly demonstrate that ROS are produced by $G\alpha_{12/13}$-mediated Rac activation, and ROS participate in JNK and p38 MAPK but not ERK activation. Previous findings indicated that Ang II stimulation produces ROS in vascular smooth muscle cells (6, 17) and suggested the role of ROS as a mediator of Ang II action (6, 14). The present study is consistent with the reports that ROS are mediators of Ang II action. We further demonstrated that the possible origin of Ang II-induced ROS production in neonatal cardiac myocytes is NADPH oxidase, because a selective inhibitor of NADPH oxidase could inhibit ROS-dependent JNK and p38 MAPK activation by Ang II stimulation.

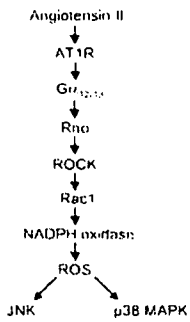

FIG. 10. **Model for ROS-dependent activation of JNK and p38 MAPK by AT1R stimulation in rat neonatal cardiac myocytes.** AT1R stimulation by angiotensin II activates $G\alpha_{12/13}$ protein. The activated $G\alpha_{12/13}$ stimulates ROS production through Rho/ROCK-mediated Rac1 activation. ROS activate JNK and p38 MAPK through with unknown mechanisms.

The expression of CA-$G\alpha_{12}$ and CA-$G\alpha_{13}$ activates all three MAPKs in rat cardiac myocytes (Fig. 5). This result is partly supported by the report that $G\alpha_{12}$ activates JNK specifically through the stimulation of MKK7, an upstream kinase of JNK (39). Furthermore, CA-$G\alpha_{12}$- or CA-$G\alpha_{13}$-induced activation of JNK and p38 MAPK was inhibited by DPI (an NADPH oxidase inhibitor). Because Ang II-induced JNK and p38 MAPK activation was significantly inhibited by catalase (an H_2O_2-degrading enzyme), we speculate the activation scheme that NADPH

oxidase-generated superoxide anion is converted to H_2O_2, and H_2O_2 forms more reactive species that participate in JNK and p38 MAPK activation machinery.

A selective EGF receptor kinase blocker AG1478 demonstrates that AT1R-stimulated JNK activation does not requires EGF receptor transactivation (Fig. 9). With cardiac fibroblasts, Murasawa *et al.* (40) reported that Ang II activates JNK through Pyk, Src, Rac, and PAK. In contrast with JNK activation, ERK activation in cardiac fibroblasts requires EGF receptor transactivation through Pyk2 and Src activation. The present study using cardiac myocytes demonstrated that Ang II-induced JNK activation was not inhibited by AG1478. We further demonstrated that Ang II-induced $G\alpha_{13}$ activation, Rho activation, Rac activation, and ROS production were not inhibited by AG1478 (Figs. 3*B* and 9). These results suggest that EGF receptor transactivation is not necessary for Ang II-induced JNK and p38 MAPK activation through $G\alpha_{12/13}$-mediated ROS production.

The present study demonstrated that Rho and ROCK positively regulate Rac activation. On the other hand, the negative regulation of Rac by Rho and ROCK has been observed by Hirose *et al.* (41). They reported that Rho/ROCK stimulated neurite retraction, and Cdc42/Rac stimulated neurite outgrowth in NIE-115 cells. They suggested that Rho/ROCK negatively regulated the Cdc42 and Rac pathway. The differential regulatory mechanism of Rac by Rho/ROCK is unknown. However, different types of RacGEF that are regulated by ROCK may express in NIE-115 and cardiac myocytes. Because we also found that a ROCK inhibitor Y27632 inhibited Ang II-induced ROS production (data not shown), the present study also suggests that ROCK mediates Ang II-induced JNK and p38 MAPK activation through Rac activation.

When cells were treated with PTX, the active form of Rac was increased even in the absence of agonist stimulation (Fig. 7*D*). The mechanism of high Rac activity by PTX treatment is unknown. One of possibilities may be mitogenic action of PTX. PTX is an A-B toxin; A-protomer is the entity that ADP-ribosylates $G\alpha_i$, and B-oligomer consists of several subunits that bind to the plasma membrane. PTX binds to cells via B-oligomer, and B-oligomer has a mitogenic activity. Therefore, the increased basal Rac activation may be caused by the mitogenic action of PTX.

DN-Rac inhibited Ang II-induced ROS production and activation of JNK and p38 MAPK. The reagents that inhibit ROS production blocked JNK and p38 MAPK activation. Thus, Rac-mediated JNK and p38 MAPK activation requires ROS. However, Rac is believed to be involved in various signaling pathways other than ROS production system (NADPH oxidase). For instance, Rac is an activator of PAK leading to JNK activation (20). We speculate that Rac activates at least two signaling pathways such as ROS production and PAK activation, and concomitant activation of two pathways is required for JNK and p38 MAPK activation.

The idea that $G_{12/13}$ proteins are involved in Ang II-mediated signaling has been also supported by some previous reports (42, 43). For example, Gohla *et al.* (42) have reported that angiotensin II stimulation increases the incorporation of azidoanilido [α-^{32}P]GTP into $G\alpha_{12}$ and $G\alpha_{13}$ in membranes of aortic smooth muscle cells. The present study substantiated their result that AT1R can directly activate $G\alpha_{13}$. We further demonstrated that inhibition of EGF receptor or $G\alpha_q$ did not affect Ang II-stimulated $G\alpha_{13}$ activation. Macrez *et al.* (43) also reported that a $\beta\gamma$ dimmer derived from G_{13} transduces AT1R signaling. Because the $\beta\gamma$-sequestering peptide GRK2-ct did not affect Ang II-induced Rac activation (Fig. 7*D*), $\beta\gamma$ derived from $G_{12/13}$ may not participate in JNK and p38 MAPK activation induced by Ang II.

$G\alpha_q$ is generally thought to mediate Ang II-induced responses. We demonstrated that expression of CA-$G\alpha_q$ activates three MAPKs in rat neonatal cardiomyocytes. However, the present study did not reveal any role of $G\alpha_q$ in Ang II receptor-stimulated JNK and p38 MAPK activation. Zou *et al.* (44) have reported that $G\alpha_q$ and protein kinase C mediate Ang II-induced ERK activation in rat cardiac myocytes. Therefore, it is reasonable to assume that the mechanism of Ang II-induced MAPK activation is different between three MAPKs; $G\alpha_q$ mediates mainly ERK activation, and $G\alpha_{12/13}$ mediates JNK and p38 MAPK activation. The blockade of JNK or p38 MAPK activation resulted in complete inhibition of Ang II-induced hypertrophic responses (32, 45). Therefore, it may be necessary to turn on multiple pathways at the same time for the full induction of hypertrophic responses upon Ang II receptor stimulation.

In summary, we have demonstrated a new signal transduction pathway of Ang II-induced JNK and p38 MAPK activation: AT1R → $G_{12/13}$ → Rho/ROCK → Rac → ROS → JNK and p38 MAPK. The signaling connection between $G\alpha_{12/13}$ and ROS in cardiac myocytes will provide a new direction of Ang II receptor-mediated signaling pathway.

Acknowledgments—We thank Drs. R. J. Lefkowitz, S. G. Rhee, K. Kaibuchi, S. Narumiya, H. Nishina, M. Simon, and M. Negishi for cDNAs encoding GRK2, PrxII, DN-Rac, C3 toxin, GST-c-Jun, $G\alpha_{12}$, $G\alpha_{13}$, and GST-TPR, respectively.

REFERENCES

1. Paradis, P., Dali-Youcef, N., Paradis, F. W., Thibault, G., and Nemer, M. (2000) *Proc. Natl. Acad. Sci. U. S. A.* **97**, 931–936
2. Schmitz, U., and Berk, B. C. (1997) *Trends. Endocrinol. Metab.* **8**, 261–266
3. Kudoh, S., Komuro, I., Mizuno, T., Yamazaki, T., Zou, Y., Shiojima, I., Takekoshi, N., and Yazaki, Y. (1997) *Circ. Res.* **80**, 139–146
4. Sadoshima, J., Qiu, Z., Morgan, J. P., and Izumo, S. (1995) *Circ. Res.* **76**, 1–15
5. Li, X., Lee, J. W., Graves, L. M., and Earp, H. S. (1998) *EMBO J.* **17**, 2574–2583
6. Ushio-Fukai, M., Alexander, R. W., Akers, M., and Griendling, K. K. (1998) *J. Biol. Chem.* **273**, 15022–15029
7. Eguchi, S., Dempsey, P. J., Frank, G. D., Motley, E. D., and Inagami, T. (2001) *J. Biol. Chem.* **276**, 7957–7962
8. Begovevitch, M. A., Glennon, P. E., Andersson, M. B., Clerk, A., Lazou, A., Marshall, C. J., Parker, P. J., and Sugden, P. H. (1994) *J. Biol. Chem.* **269**, 1110–1119
9. Sugden, P. H., and Clerk, A. (1998) *J. Mol. Med.* **76**, 725–746
10. Sadoshima, J., and Izumo, S. (1996) *EMBO J.* **15**, 775–787
11. Luttrell, L. M., Roudabush, F. L., Choy, E. W., Miller, W. E., Field, M. E., Pierce, K. L., and Lefkowitz, R. J. (2001) *Proc. Natl. Acad. Sci. U. S. A.* **98**, 2449–2454
12. Abe, J., and Berk, B. C. (1998) *Trends. Cardiovasc. Med.* **8**, 59–64
13. Takemoto, M. Node, K. Nakagomi, H. Liao, Y. Grimm, M., Takemoto, Y., Kitakaze, M., and Liao, J. K. (2001) *J. Clin. Investig.* **108**, 1429–1437
14. Griendling, K. K., and Ushio-Fukai, M. (2000) *Regul. Pept.* **91**, 21–27
15. Nishida, M., Maruyama, Y., Tanaka, R., Kontani, K., Nagao, T., and Kurose, H. (2000) *Nature* **408**, 492–495
16. Nishida, M., Schey, K. L., Takagahara, S., Kontani, K., Katada, T., Urano, Y., Nagano, T., Nagao, T., and Kurose, H. (2002) *J. Biol. Chem.* **277**, 9036–9042
17. Rajagopalan, S., Kurz, S., Münzel, T., Tarpey, M., Freeman, B. A., Griendling, K. K., and Harrison, D. G. (1996) *J. Clin. Investig.* **97**, 1916–1923
18. Griendling, K. K., Minieri, C. A., Ollerenshaw, J. D., and Alexander, R. W. (1994) *Circ. Res.* **74**, 1141–1148
19. Bokoch, G. M., and Knaus, U. G. (2003) *Trends Biochem. Sci.* **28**, 502–508
20. Schmitzs, U., Thömmes, K., Beier, I., Wagner, W., Sachinidis, A., Düsing, R., and Vetter, H. (2001) *J. Biol. Chem.* **276**, 22003–22010
21. Nishida, M., Nagao, T., and Kurose, H. (1999) *Biochem. Biophys. Res. Commun.* **262**, 350–354
22. Coso, O. A., Chiariello, M., Yu, J.-C., Teramoto, H., Crespo, P., Xu, N., Miki, T., and Gutkind, J. S. (1995) *Cell* **81**, 1137–1146
23. Minden, A., Lin, A., McMahon, M., Lange-Carter, C. Dérijard, B., Davis, R. J., Johnson, G. L., and Karin M. (1994) *Science* **266**, 1719–1723
24. Minden, A., Lin, A., Claret, F.-X., Abo, A., and Karin, M. (1995) *Cell* **81**, 1147–1157
25. Kurose, H. (2003) *Life Sci.* **74**, 155–161
26. Kozasa, T., Jiang, X., Hart, M. J., Sternweis, P. M., Singer, W. D., Gilman, A. G., Bollag, G., and Sternweis, P. C. (1998) *Science* **280**, 2109–2111
27. Hart, M. J., Jiang, X., Kozusa, T., Roscoe, W., Singer W. D., Gilman, A. G., Sternweis, P. C., and Bollag, G. (1998) *Science* **280**, 2112–2114
28. Shiina, T., Arai, K., Tanabe, S., Yoshida, N., Hugu, T., Nagao, T., and Kurose, H. (2001) *J. Biol. Chem.* **276**, 33019–33026
29. Kurose, H., Arrizn, J. L., and Lefkowitz, R. J. (1993) *Mol. Pharmacol.* **43**, 444–450
30. He, T.-C., Zhou, S., Da Costa, L. T., Yu, J., Kinzler, K. W., and Vogelstein, B. (1998) *Proc. Natl. Acad. Sci. U. S. A.* **95**, 2509–2514
31. Miyake, S., Makimura, M., Kanegae, Y., Harada, S., Sato, Y., Takamuri, K.,

Tokuda, C., and Saito, I. (1996) *Proc. Natl. Acad. Sci. U. S. A.* **93**, 1320–1324
32. Maruyama, Y., Nishida, M., Sugimoto, Y., Tanabe, S., Turner, J. H., Kozasa, T., Wada, T., Nagao, T., and Kurose, H. (2002) *Circ. Res.* **91**, 961–969
33. Arai, K., Maruyama, Y., Nishida, M., Tanabe, S., Takagahara, S., Kozasa, T., Mori, Y., Nagao, T., and Kurose, H. (2003) *Mol. Pharmacol.* **63**, 478–488
34. Kang, S. W., Chae, H. Z., Seo, M. S., Kim, K., Baines, I. C., and Rhee, S. G. (1998) *J. Biol. Chem.* **273**, 6297–6302
35. Ren, X.-D., and Schwartz, M. A. (2000) *Methods Enzymol.* **325**, 264–272
36. Yamaguchi, Y., Katoh, H., and Negishi, M. (2003) *J. Biol. Chem.* **278**, 14936–14939
37. Clerk, A., Pham, F. H., Fuller, S. J., Sahai, E., Aktories, K., Marais, R., Marshall, C., and Sugden, P. H. (2001) *Mol. Cell. Biol.* **21**, 1173–1184
38. Matsui, T., Amano, M., Yamamoto, T., Chihara, K., Nakafuku, M., Ito, M., Nakano, T., Okawa, K., Iwamatsu, A., and Kaibuchi, K. (1996) *EMBO J.* **15**, 2208–2216
39. Dermott, J. M., Ha, J. H., Lee, C. H., and Dhanasekaran, N. (2004) *Oncogene* **23**, 226–232
40. Murasawa, S., Matsubara, H., Mori, Y., Masaki, H., Tsutsumi, Y., Shibasaki, Y., Kitabayashi, I., Tanaka, Y., Fujiyama, S., Koyama, Y., Fujiyama, A., Iba, S., and Iwasaka, T. (2000) *J. Biol. Chem.* **275**, 26856–26863
41. Hirose, M. Ishizaki, T. Watanabe, N., Uehata, M., Kranenburg, O., Moolenaar, W. H., Matsumura, F., Maekawa, M., Bito, H., and Narumiya, S. (1998) *J. Cell Biol.* **141**, 1625–1636
42. Gohla, A., Schultz, G., and Offermanns, S. (2000) *Circ. Res.* **87**, 221–227
43. Macrez, N., Morel, J-L., Kalkbrenner, F., Viard, P., Schultz, G., and Mironneau, J. (1997) *J. Biol. Chem.* **272**, 23180–23185
44. Zou, Y., Komuro, I., Yamazaki, T., Kudoh, S., Aikawa, R., Zhu, W., Shiojima, I., Hiroi, Y., Tobe, K., Kadowaki, T., and Yazaki, Y. (1998) *Circ. Res.* **82**, 337–345
45. Reddy, M. A., Thimmalapura, P.-R., Lanting, L., Nadler, J., L., Fatima, S., and Natarajan, R. (2002) *J. Biol. Chem.* **277**, 9920–9928

Expression of Annexin A3 in Primary Cultured Parenchymal Rat Hepatocytes and Inhibition of DNA Synthesis by Suppression of Annexin A3 Expression Using RNA Interference

Shingo NIIMI,*[a] Mizuho HARASHIMA,[b] Masaru GAMOU,[b] Masashi HYUGA,[a] Taiichiro SEKI,[b] Toyohiko ARIGA,[b] Toru KAWANISHI,[a] and Takao HAYAKAWA[c]

[a] *Division of Biological Chemistry and Biologicals, National Institute of Health Sciences; 1–18–1 Kamiyoga, Setagaya-ku, Tokyo 158–8501, Japan;* [b] *Department of Nutrition and Physiology, Nihon University College of Bioresource Sciences; Kameino, Fujisawa 252–8510, Japan; and* [c] *Deputy Director General, National Institute of Health Sciences; 1–18–1 Kamiyoga, Setagaya-ku, Tokyo 158–8501, Japan.*

Received October 30, 2004; accepted January 5, 2005; published online January 7, 2005

Annexin A3 is a member of the lipocortin/annexin family, which binds to phospholipids and membranes in a Ca^{2+}-dependent manner. Although annexin A3 has various functions *in vitro*, its cellular significance is completely unknown. Annexin A3 is not found in rat liver *in vivo*. In the present study, we investigated the expression of annexin A3 in primary cultured parenchymal rat hepatocytes. Annexin A3 protein was detected in 48-h, but not 2.5-h, cultured hepatocytes using Western blot analysis. The annexin A3 level further increased after an additional 24 h of culture. Annexin A3 mRNA was not detected in 2.5-h cultured hepatocytes but was detected 22 h after the start of culture by RT-PCR analysis, reaching a maximum value after 48 h of culture. To define the role of Annexin A3 in DNA synthesis, RNA interference was used to reduce annexin III gene expression in hepatocytes. The transfection of small interfering RNAs targeting annexin A3 in the hepatocytes reduced the corresponding mRNA and protein expression by approximately 80% and more than 90%, respectively, at 24 h after transfection. In the annexin A3 small interfering RNAs-transfected cells, DNA synthesis, as assessed by [^{3}H]thymidine incorporation, decreased by approximately 70% not only in the control cultures, but also in the hepatocyte growth factor- or epidermal growth factor-treated cells. These findings show that annexin A3 is expressed in primary cultured parenchymal rat hepatocytes and that the suppression of annexin A3 expression using RNA interference inhibits DNA synthesis.

Key words annexin A3; RNAi; DNA synthesis; primary cultured hepatocyte; hepatocyte growth factor (HGF); epidermal growth factor (EGF)

Annexin (Anx) A3 is also called "lipocortin 3" or "placental anticoagulant protein 3" (PAP-III)[1] and is a member of the lipocortin/annexin family, which binds to phospholipids and membranes in a Ca^{2+}-dependent manner.[2—4] AnxA3 has been shown to have anticoagulant and anti-phospholipase A_2 properties *in vitro*[5] and to promote the Ca^{2+}-dependent aggregation of isolated specific granules from human neutrophils.[6] Although the physiological functions of other annexins have been recently clarified in knock-out and transgenic models,[7—14] the functions of AnxA3 are completely unknown.[15]

Recently, we found that AnxA3 protein and its mRNA are not expressed in isolated parenchymal rat hepatocytes.[16,17] Consistent with these findings, AnxA3 protein and its mRNA are not detectable by Western blot analysis and Northern blot analysis in rat liver.[18—21] However, there have been no reports on the behavior of AnxA3 in primary cultured parenchymal rat hepatocytes. In the present study, we investigated the expression and function of AnxA3 in cultured parenchymal rat hepatocytes.

MATERIALS AND METHODS

Materials Recombinant human hepatocyte growth factor (HGF) was purchased from R&D systems (Minneapolis, MN, U.S.A.). Mouse epidermal growth factor (EGF) was purchased from Wako (Osaka, Japan). [^{3}H]thymidine (79.9 Ci/mmol) was purchased from PerkinElmer (Boston, MA, U.S.A.). Rabbit anti-human ANXA3 antibody serum was a generous gift from Dr. F. Russo-Marie and Dr. C. Raguenness-Nicol.

Cell Isolation and Monolayer Cultures Parenchymal hepatocytes were isolated from adult male Wistar rats, weighing 180—200 g, by *in situ* perfusion of the liver with collagenase.[22] All animal care and procedure protocols were approved by the institutional care committee. The cells were then suspended at a density of 2.5×10^5 cells/ml in Williams E medium (WE) containing 5% fetal bovine serum and 1 nM insulin and cultured at a density of 0.5×10^5 cells/cm^2 in a 6 cm dish and a 48-well microplate precoated with collagen type-I AC in a humidified chamber at 37 °C in 5% CO_2 and 30% O_2 in air. Cells plated in the 6-cm dish and 48-well microplate were used to prepare total cellular extracts or total RNA and to measure DNA synthesis, respectively. After 2.5 h of culture, the medium was replaced with a serum- and hormone-free medium containing aprotinin (1 μg/ml).

Western Blot Analysis Cell lysates were prepared using a modification of a previously described method.[23] The cells were washed with phosphate-buffered saline (PBS) followed by buffer A (50 mM Tris–HCl [pH 7.5], 150 mM NaCl, and 10 mM EDTA). The cells were then harvested after the addition of 20 μl of buffer A. The cells were suspended, shaken for 15 min at room temperature, and sonicated five times for 15 s each time while in an ice bath after the addition of 1/5 [v/v] of 5×buffer A containing 2.5% Triton X-100 and 1/100 [v/v] of a protease inhibitor cocktail (SIGMA). After centrifugation at $100000\times g$, the cytosolic fraction (about 25 μg) was subjected to sodium dodecyl sulfate-polyacrylamide gel

* To whom correspondence should be addressed. e-mail: niimi@nihs.go.jp

electrophoresis on a 10% gel and electroblotted to a PVDF membrane (GVHP; Millipore). After blocking the membrane with 5% skimmed milk, a Western blot analysis was performed using rabbit anti-human AnxA3 antibody serum at a dilution of 1 : 18000; detection was performed using the ECL detection system (Amersham Bioscience).

Reverse Transcription Polymerase Chain Reaction Analysis Total RNA was exctracted from the cells using Trizol reagent (Invitrogen) according to the manufacturer's protocols. Approximately 3 μg of RNA per sample was reverse-transcribed using the THERMOSCRIPT™ RT-PCR System (Invitrogen) and oligo$(dT)_{20}$ in a final volume of 40 μl, according to the manufacturer's protocols. Subsequently, 1 μl of cDNA was polymerase chain reaction (PCR)-amplified using the THERMOSCRIPT™ RT-PCR System (Invitrogen) in a final volume of 20 μl per reaction, according to the manufacturer's protocols, for 14—23 cycles of denaturation for 30 s at 94 °C, annealing for 30 s at 60 °C, and polymerization for 1 min at 72 °C using Anx AIII or glyceraldehyde 3-phosphate dehydrogenase (GAPDH) cDNA specific primers under linear conditions. The PCR products were separated on a 2% agarose gel, stained with SYBR Green I, and visualized and analyzed with a FluorolmagerSS 595 (Amersham Bioscience). A computer assisted-analyzer was used to quantitatively analyze the signals, and the signals were normalized to the signal of a house keeping gene, the gene coding GAPDH. The sequences of the AnxA3 primers were as follows: 5'-CAAATTCACCGAGATCCTGT-3' and 5'-TGCTGGAGTGCTGTACGAAA-3'. The sequences of the GAPDH primers were as follows: 5'-ACCACAGTCCATGCCATCAC-3' and 5'-TCCACCACCTGTTGCTGTA-3'.[24] The PCR product specificity was confirmed by DNA sequence analysis using an ABI Prism 377 DNA Sequencer (Applied Biosystems, Foster City, CA, U.S.A.).

Preparation and Transfection of Small Interfering RNAs Targeting AnxA3 Small interfering RNAs (siRNAs) targeting rat AnxA3 were designed according to the guidelines of the "Dharmacon siDESIGN Center" (www.dharmacon.com) and obtained from Dharmacon Research (Lafayette) in annealed and lyophilized forms. The target sequences were localized at positions, 493 and 690 bps downstream of the start codon. The sequences of each siRNA pair were as follows: AnxA3 siRNA 1, 5'-GAG ACG AAA GCC UGA AAG UdTdT-3' and ACU UUC AGG CUU UCG UCU cdTdT-3'; ANXA3 siRNA 2, 5'-GGA GAA UUA UCU GGG CAU UdTdT-3' and AAU GCC CAG AUA AUUCUC cdTdT-3; and control siRNA, 5'-ACU CUA UCU GCA CGC UGA CUU-3' and 5'-P G UCA GCG UGC AGA UAG AGU UU-3'. No homology between any relevant mammalian gene and the control siRNA was observed. These siRNAs were dissolved in an RNase-free solution provided by Dharmacon Research at a concentration of 20 μM. After 20 h of cell culture, the medium was replaced with WE containing aprotinin (1 μg/ml) immediately prior to transfection. Transfection with siRNA was performed using SiFector (B-bridge), according to the user guidelines. Sixty microliters of both AnxA3 siRNA 1 and 2 were diluted with OPTI-MEM (Invitrogen) to a final volume of 400 μl. Sixty-four microliters of SiFector was also diluted in OPTI-MEM to a final volume of 400 μl, then suspended and incubated at room temperature for 5 min. Next, the diluted siRNA was combined with SiFector, and the mixture was incubated at room temperature to allow the siRNA-SiFector complex to form. Eight hundred microliters of the siRNA-SiFector complex was added to the cultures (6-cm dish). For the 48-well plates, the siRNA-SiFector complex was prepared as described above except that the volume of each solution per well was scaled down to 1/16.

Measurement of [^{3}H]thymidine Incorporation After 20 h of culture, the medium was replaced with hormone-free medium containing aprotinin (1 μg/ml) and 0.1% bovine serum albumin (BSA), and EGF (2 ng/ml) or HGF (20 ng/ml) was added. After 1 h, 50 μl of siRNA-SiFector complex, prepared as described above, was added to the wells. After another 24 h, [^{3}H]thymidine (0.626 μCi) and thymidine (676.6 ng) were added, and 10 μg/ml of aphidicolin was added to some wells at the same time. The cells were then cultured for another 24 h. [^{3}H]thymidine incorporation was measured as described previously.[25] The difference between the radioactivity in the hot-trichloroacetic acid soluble fraction with and without aphidicolin was calculated as dpm/mg protein. Cell protein was measured using a previously described method,[26] with BSA used as a standard.

RESULTS

Expression of AnxA3 during Culture At first, we investigated the expression of AnxA3 in primary cultured parenchymal rat hepatocytes. AnxA3 protein was not detected by Western blot analysis 2.5 and 24 h after the start of culture but was detected after 48 h of culture (Fig. 1A). The level after 72 h of culture was approximately 1.6-fold higher than that after 48 h of culture (Fig. 1B). AnxA3 mRNA was not detected by reverse transcription (RT)-PCR in cultured hepatocytes after 2.5 h of culture but was significantly detected after 22 h of culture (Fig. 2A), reaching a maximum value after 48 h of culture (Fig. 2B). These results indicate

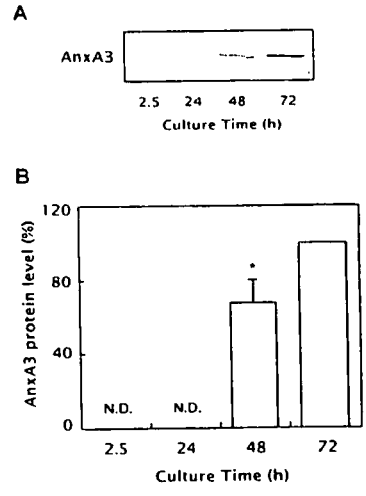

Fig. 1. Expression of AnxA3 Protein during Culture

(A) The data shown are representative of the Western blot analysis results. Cells lysates were prepared from the cells at the indicated times and used for the Western blot analysis. (B) The intensity of each band was quantified, and the results are shown relative to the value of cells cultured for 72 h. The data are expressed as the mean±S.D. of 3 experiments. *$p<0.01$, compared with the value of cells cultured for 72 h. N.D., not detected.

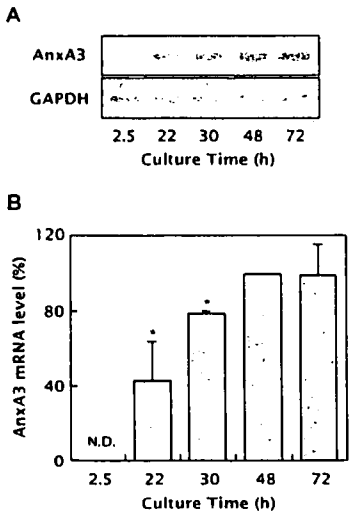

Fig. 2. Increase in AnxA3 mRNA Level during Culture

(A) The data shown are representative of the RT-PCR analysis results. Total RNA was prepared from the cells at the indicated times and used for the RT-PCR analysis. (B) The intensity of each band was quantified, and the results are shown relative to the value of cells cultured for 48 h. The data are expressed as the mean±S.D. of 3 experiments. *$p<0.01$, compared with the value of cells cultured for 48 h. N.D., not detected.

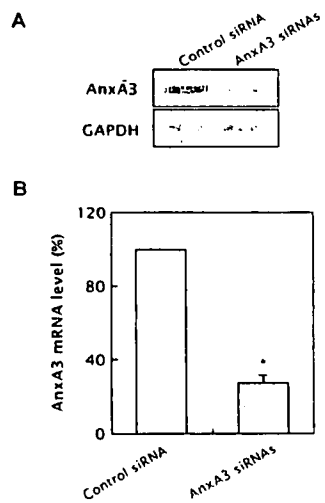

Fig. 3. Suppression of Increase in AnxA3 mRNA Level during Culture with RNAi

(A) The data shown are representative of the RT-PCR analysis results. Total RNA was prepared from the cells 1 d after siRNA transfection and used for the RT-PCR analysis. (B) The intensity of each band was quantified, and the results are shown relative to the value of cells transfected with control siRNA. The data are expressed as the mean±S.D. of 3 experiments. *$p<0.01$, compared with the value of cells transfected with control siRNA.

that the expression of AnxA3 is regulated by its mRNA level.

Suppression of AnxA3 Expression Using RNA Interference Next, we attempted to suppress AnxA3 expression by RNA interference (RNAi) to examine the role of ANXA3 in the cultured hepatocytes. AnxA3 mRNA expression was markedly reduced by treatment with AnxA3 siRNAs, compared with the expression after treatment with control siRNA, 1 d after the transfection (Fig. 3A), with an inhibition of approximately 80% (Fig. 3B). Furthermore, the AnxA3

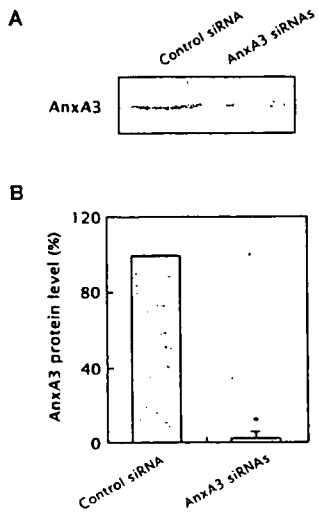

Fig. 4. Suppression of AnxA3 Protein Expression during Culture with RNAi

(A) The data shown are representative of the Western blot analysis results. Cells lysates were prepared from the cells 1 d after siRNA transfection and used for the Western blot analysis. (B) The intensity of each band was quantified, and the results are shown relative to the value of cells transfected with control siRNA. The data are expressed as the mean±S.D. of 3 experiments. *$p<0.01$, compared with the value of cells transfected with control siRNA.

protein level was also reduced by the treatment with AnxA3 siRNAs compared with the level after treatment with control siRNA (Fig. 4A), with an inhibition of more than 95% (Fig. 4B). On the other hand, the control siRNA had almost no effect on AnxA3 protein and mRNA levels compared with those treated with SiFector alone (data not shown). Neither the control nor AnxA3 siRNAs caused any cytotoxic effects, as observed microscopically or by the quantification of the total amount of protein in each sample (data not shown). These results indicate that AnxA3 siRNAs efficiently and specifically, inhibit the expression of AnxA3 in primary cultured parenchymal rat hepatocytes.

Inhibition of DNA Synthesis by Suppression of AnxA3 Expression Using RNAi Finally, we examined the role of AnxA3 in DNA synthesis by suppressing AnxA3 expression using RNAi. EGF (2 ng/ml) and HGF (20 ng/ml) stimulated DNA synthesis by approximately 7-fold and 9-fold, respectively in hepatocytes treated with control siRNA (Fig. 5). The stimulations were inhibited to approximately 70% by treatment with AnxA3 siRNAs. Similar results were also obtained in the control cells, whereas the control siRNA had almost no effect on DNA synthesis, compared with the effect in cells treated with SiFector alone (data not shown).

DISCUSSION

In the present study, we showed for the first time that AnxA3 is expressed in cultured parenchymal rat hepatocytes and that the inhibition of AnxA3 expression by RNAi resulted in a significant inhibition of DNA synthesis, suggesting that the expression of AnxA3 is necessary for DNA synthesis in primary cultured parenchymal rat hepatocytes.

Hepatocytes placed under culture conditions, are known to acquire a growth potential characterized by the enhancement of DNA synthesis, which is caused by several growth

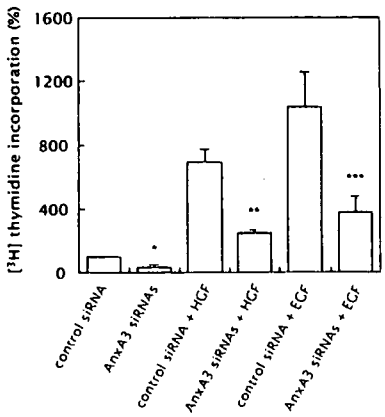

Fig. 5. Inhibition of DNA Synthesis by RNAi

The results are shown relative to the value of control cultured cells transfected with control siRNA. The data are expressed as the mean±S.D. of duplicate wells in 3 experiments. *$p<0.01$, compared with the value of control cultured cells transfected with control siRNA. **$p<0.01$, compared with the value of cells cultured in the presence of HGF and transfected with control siRNA. ***$p<0.01$, compared with the value of cells cultured in the presence of EGF and transfected with control siRNA. The mean±S.D. of [³H]thymidine incorporation in the control cultured cells transfected with control siRNA was $9.72\times10^4\pm0.68\times10^4$ dpm/mg protein.

factors.[27,28] Our present findings suggest that the expression of AnxA3 is partly necessary for hepatocytes to acquire a growth potential under culture conditions. In fact, the enhanced expression of AnxA3 has been observed in hepatocellular carcinoma cell lines.[29] In addition, we discovered that the enhanced expression of Anx3 was observed in the proliferative hepatocytes after carbon tetrachloride-induced rat liver damage (unpublished observations).

As for other annexins, several findings concerning the relation of AnxA1 to hepatocyte growth has been reported as described below. The suppression of AnxA1 expression using antisense technology inhibited proliferation in a mouse hepatocyte cell line.[30] AnxA1 increased in the proliferative hepatocytes after carbon tetrachloride-induced rat liver damage or a partial hepatectomy and in hepatocellullar carcinoma tissue.[31,32]

Although the mechanism of action of AnxA3 on DNA synthesis is presently uncertain, the target of AnxA3 may be a common signal transduction pathway, and not necessarily a constitutive or growth factor-mediated one, because the suppression of AnxA3 expression using RNAi not only inhibited the control of DNA synthesis, but also EGF- or HGF-stimulated DNA synthesis, almost to a similar level. In this respect, the findings described below may be relevant to speculations on the mechanism of action of AnxA3 on DNA synthesis. The growth factor-mediated enhancement of hepatocyte growth consists of several signal transduction pathways.[33] The activation of cytosolic phospholipase A_2 ($cPLA_2$) by MAP kinase liberates arachidonic acid from phospholipids and is followed by the generation of prostaglandins, mediators of DNA synthesis, *via* cyclooxygenase. Interestingly, the suppression of AnxA1 expression using antisense technology inhibited $cPLA_2$ activity in a mouse hepatocyte cell line.[30] This report suggests that $cPLA_2$ must be phosphorylated by AnxA1 to become active. Additional evidence suggests that AnxA1 (275—346 aa), the region responsible for phospholipid binding is necessary for the interaction between AnxA1 and $cPLA_2$.[34] Further study is required to clarify the mechanism of action of AnxA3, including the possibility that AnxA3 positively modulates $cPLA_2$ activity, as in the case of AnxA1.

Acknowledgements This work was supported by grants for Health and Welfare Research from the Japanese Ministry of Health, Labor and Welfare.

REFERENCES

1) Crumpton M. J., Dedman J. R., *Nature* (London), **345**, 212 (1990).
2) Raynal P., Pollard H. B., *Biochim. Biophys. Acta*, **1197**, 63—93 (1994).
3) Gerke V., Moss S. E., *Physiol. Rev.*, **82**, 331—371 (2002).
4) Moss S. E., Morgan R. O., *Genome Biol.*, **5**, 219. 1—8 (2004).
5) Tait J. F., Sakata M., McMullen B. A., Miao C. H., Funakoshi T., Hendrickson L. E., Fujikawa K., *Biochemistry*, **27**, 6268—6276 (1988).
6) Ernst J. D., Hoye E., Blackwood R. A., Jaye D., *J. Clin. Invest.*, **85**, 1065—1071 (1990).
7) Guntcski-Hamblin A. M., Song G., Walsh R. A., Frenzke M., Boivin G. P., Dorn G. W., 2nd, Kaetzel M. A., Horseman N. D., Dedman J. R., *Am. J. Physiol.*, **270**, H1091—1100 (1996).
8) Kubista H., Hawkins T. E., Patel D. R., Haigler H. T., Moss S. E., *Curr. Biol.*, **9**, 1403—1406 (1999).
9) Srivastava M., Atwater I., Glasman M., Leighton X., Goping G., Caohuy H., Miller G., Pichel J., Westphal H., Mears D., Rojas E., Pollard H. B., *Proc. Natl. Acad. Sci. U.S.A.*, **96**, 13783—13788 (1999).
10) Herr C., Smyth N., Ullrich S., Yun F., Sasse P., Hescheler J., Fleischmann B., Lasek K., Brixius K., Schwinger R. H., Fassler R., Schroder R., Noegel A. A., *Mol. Cell. Biol.*, **21**, 4119—4128 (2001).
11) Song G., Harding S. E., Duchen M. R., Tunwell R., O'Gara P., Hawkins T. E., Moss S. E., *Faseb. J.*, **16**, 622—624 (2002).
12) Roviezzo F., Getting S. J., Paul-Clark M. J., Yona S., Gavins F. N., Perretti M., Hannon R., Croxtall J. D., Buckingham J. C., Flower R. J., *J. Physiol. Pharmacol.*, **53**, 541—553 (2002).
13) Hannon R., Croxtall J. D., Getting S. J., Roviezzo F., Yona S., Paul-Clark M. J., Gavins F. N., Perretti M., Morris J. F., Buckingham J. C., Flower R. J., *Faseb. J.*, **17**, 253—255 (2003).
14) Croxtall J. D., Gilroy D. W., Solito E., Choudhury Q., Ward B. J., Buckingham J. C., Flower R. J., *Biochem. J.*, **371**, 927—935 (2003).
15) Rand J. H., *N. Engl. J. Med.*, **340**, 1035—1036 (1999).
16) Niimi S., Hyuga M., Harashima M., Seki T., Ariga T., Kawanishi T., Hayakawa T., *Biol. Pharm. Bull.*, **27**, 1864—1868 (2004).
17) Niimi S., Oshizawa T., Yamaguchi T., Harashima M., Seki T., Ariga T., Kawanishi T., Hayakawa T., *Biochem. Biophys. Res. Commun.*, **300**, 770—774 (2003).
18) Kaetzel M. A., Hazarika P., Dedman J. R., *J. Biol. Chem.*, **264**, 14463—14470 (1989).
19) Comera C., Rothhut B., Cavadore J. C., Vilgrain I., Cochet C., Chambaz E., Russo-Marie F., *J. Cell. Biochem.*, **40**, 361—370 (1989).
20) Kristensen B. I., Kristensen P., Johnsen A. H., *Int. J. Biochem.*, **25**, 1195—1202 (1993).
21) Pepinsky R. B., Tizard R., Mattaliano R. J., Sinclair L. K., Miller G. T., Browning J. L., Chow E. P., Burne C., Huang K. S., Pratt D., Wachter L., Hession C., Frey A. Z., Wallner B. P., *J. Biol. Chem.*, **263**, 10799—10811 (1988).
22) Tanaka K., Sato M., Tomita Y., Ichihara A., *J. Biochem.* (Tokyo), **84**, 937—946 (1978).
23) Romisch J., Schuler E., Bastian B., Burger T., Dunkel F. G., Schwinn A., Hartmann A. A., Paques E. P., *Blood Coagul. Fibrinolysis*, **3**, 11—17 (1992).
24) Uno S., Nakamura M., Seki T., Ariga T., *Biochem. Biophys. Res. Commun.*, **239**, 123—128 (1997).
25) Niimi S., Horikawa M., Seki T., Ariga T., Kobayashi T., Hayakawa T., *Biol. Pharm. Bull.*, **25**, 437—440 (2002).
26) Bradford M. M., *Anal. Biochem.*, **72**, 248—254 (1976).
27) Fausto N., Laird A. D., Webber E. M., *Faseb. J.*, **9**, 1527—1536 (1995).
28) Michalopoulos G. K., DeFrances M. C., *Science*, **276**, 60—66 (1997).
29) Liang R. C., Neo J. C., Lo S. L., Tan G. S., Seow T. K., Chung M. C., *J. Chromatogr. B Analyt. Technol. Biomed. Life Sci.*, **771**, 303—328 (2002).
30) de Coupade C., Gillet R., Bennoun M., Briand P., Russo-Marie F.,

Solito E., *Hepatology*, **31**, 371—380 (2000).
31) Masaki T., Tokuda M., Fujimura T., Ohnishi M., Tai Y., Miyamoto K., Itano T., Matsui H., Watanabe S., Sogawa K., Yamada T., Konishi R., Nishioka M., Hatase O., *Hepatology*, **20**, 425—435 (1994).
32) Masaki T., Tokuda M., Ohnishi M., Watanabe S., Fujimura T., Miyamoto K., Itano T., Matsui H., Arima K., Shirai M., Maeba T., Sogawa K., Konishi R., Taniguchi K., Hatanaka Y., Hatase O., Nishioka M., *Hepatology*, **24**, 72—81 (1996).
33) Adachi T., Nakashima S., Saji S., Nakamura T., Nozawa Y., *Hepatology*, **21**, 1668—1674 (1995).
34) Kim S. W., Rhee H. J., Ko J., Kim Y. J., Kim H. G., Yang J. M., Choi E. C., Na D. S., *J. Biol. Chem.*, **276**, 15712—15719 (2001).